NCREE Mini-Symposium

Topographic Effects in Strong Ground Motions

Manisha Rai
Adrian Rodriguez-Marek

Department of Civil and Environmental Engineering
Virginia Tech

Taipei, July 31 2019

Outline

- Background
- Objective
- Analysis Methodology
- Results
- Conclusions

Background

- Amplification of ground motions on ridges and hills, and deamplification on depressions
- Alternating amplification and deamplification on flanks of a slope
- Frequency dependent – inversely proportional to feature dimension

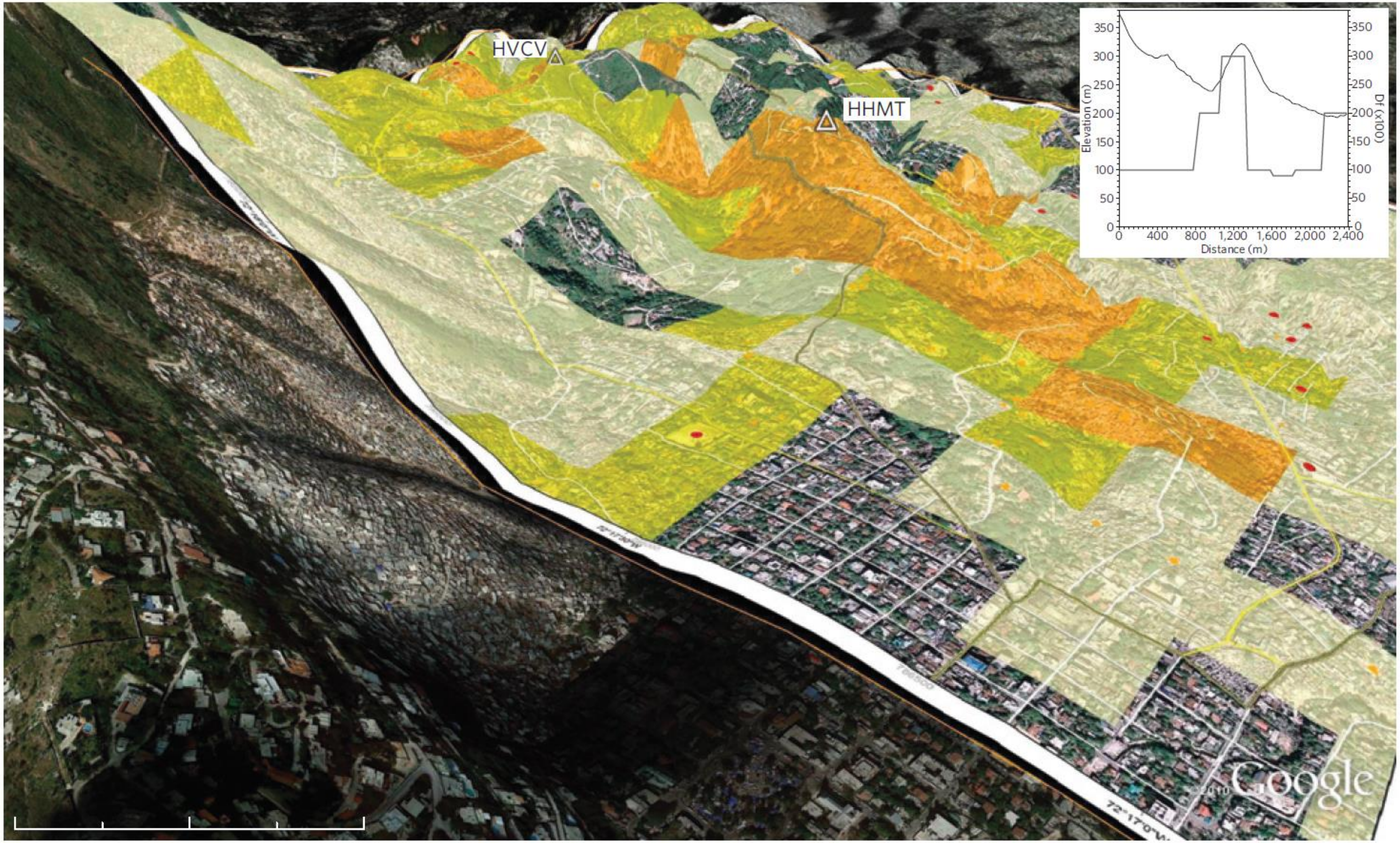

Damage in Pietonville District during the Haiti Earthquake. Heavy damage in Orange; light damage in beige (Hough et al. 2010)

Instrumented Case Histories

San Fernando Earthquake, California
Mw = 6.6, 1971

Pacoima Dam Abbutment
R_{cl} = 1.8 km

1.25 g horizontal

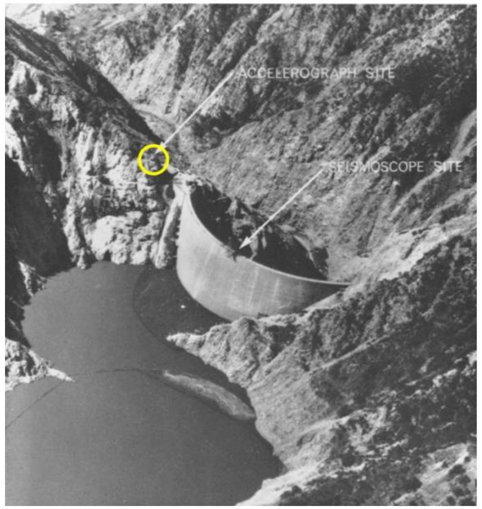

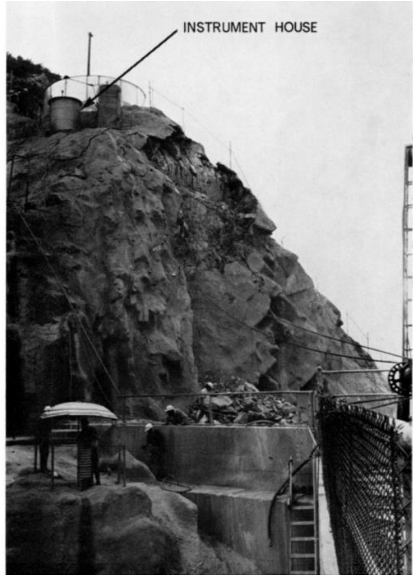

[Trifunac & Hudson, 1971]
[Boore, 1972]
[Bouchon, 1973]

Northridge Earthquake, California
Mw = 6.7, 1994

Tarzana GM Station
R_{cl} = 15.6 km

1.78 g horizontal
1.2 g vertical

Aftershock Records

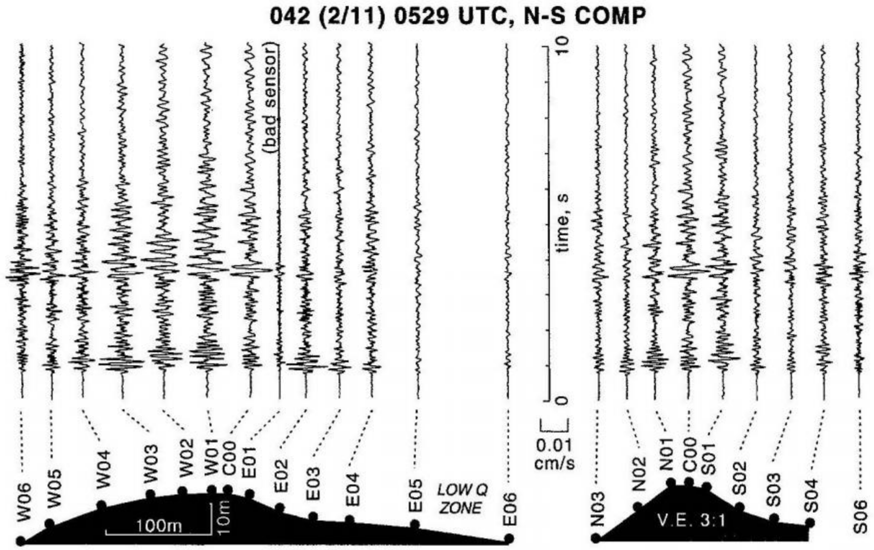

[Spudich *et al.*, 1996]

Courtesy of Emeline Maufroy

VirginiaTech Invent the Future®

Background

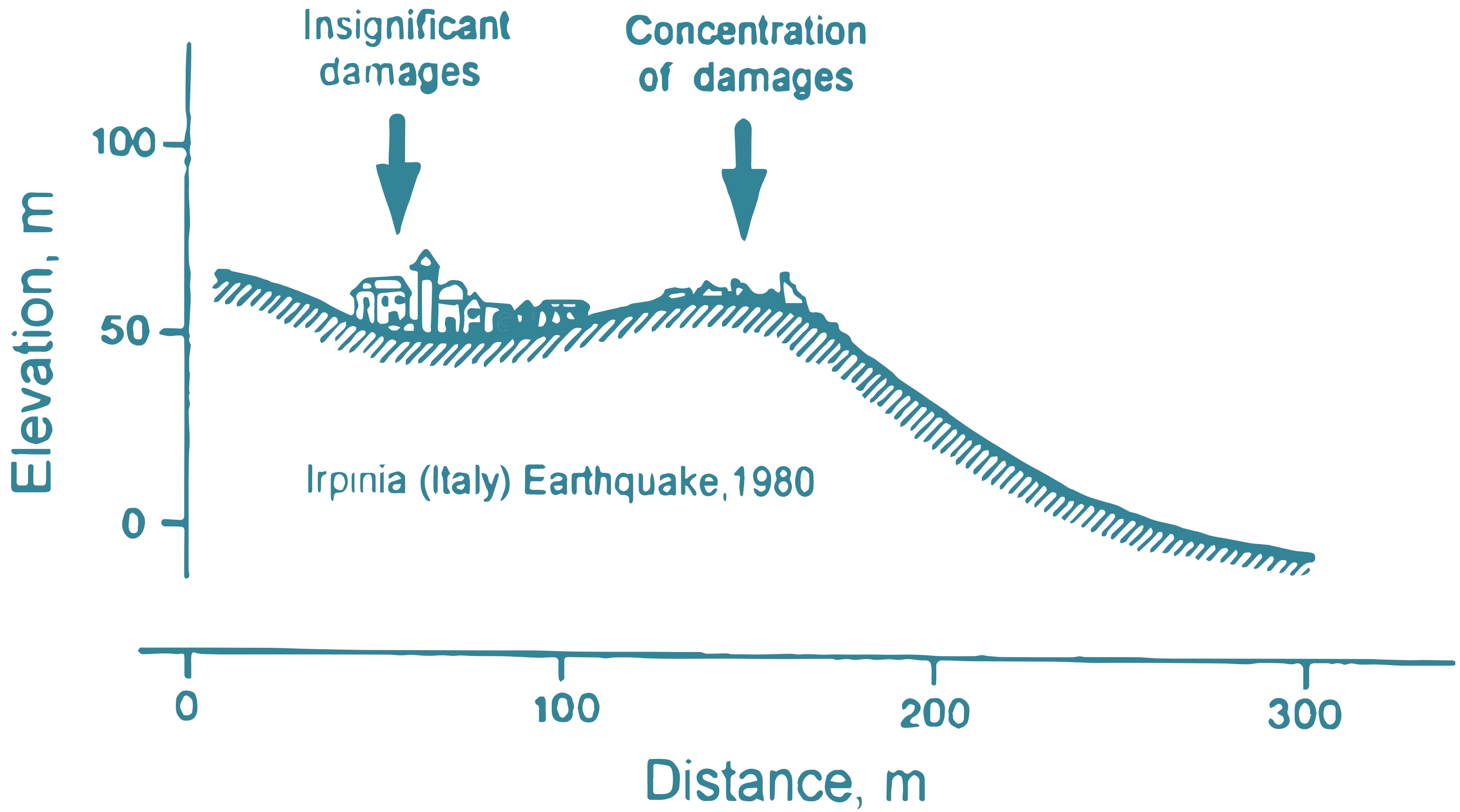

From Athanasopoulos et al. (1999)

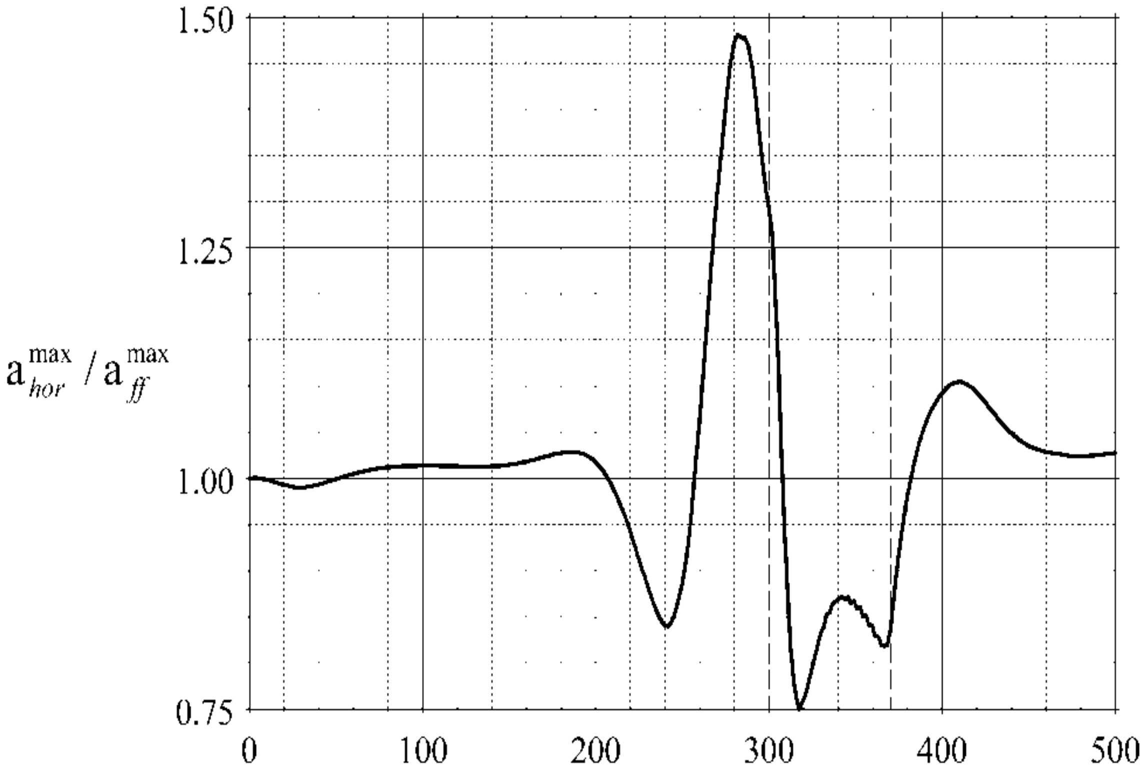

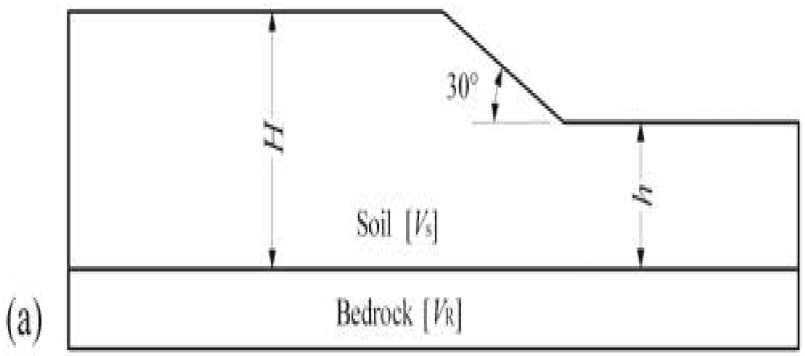

Normalized acceleration along a homogeneous slope (Assimaki et al. 1999)

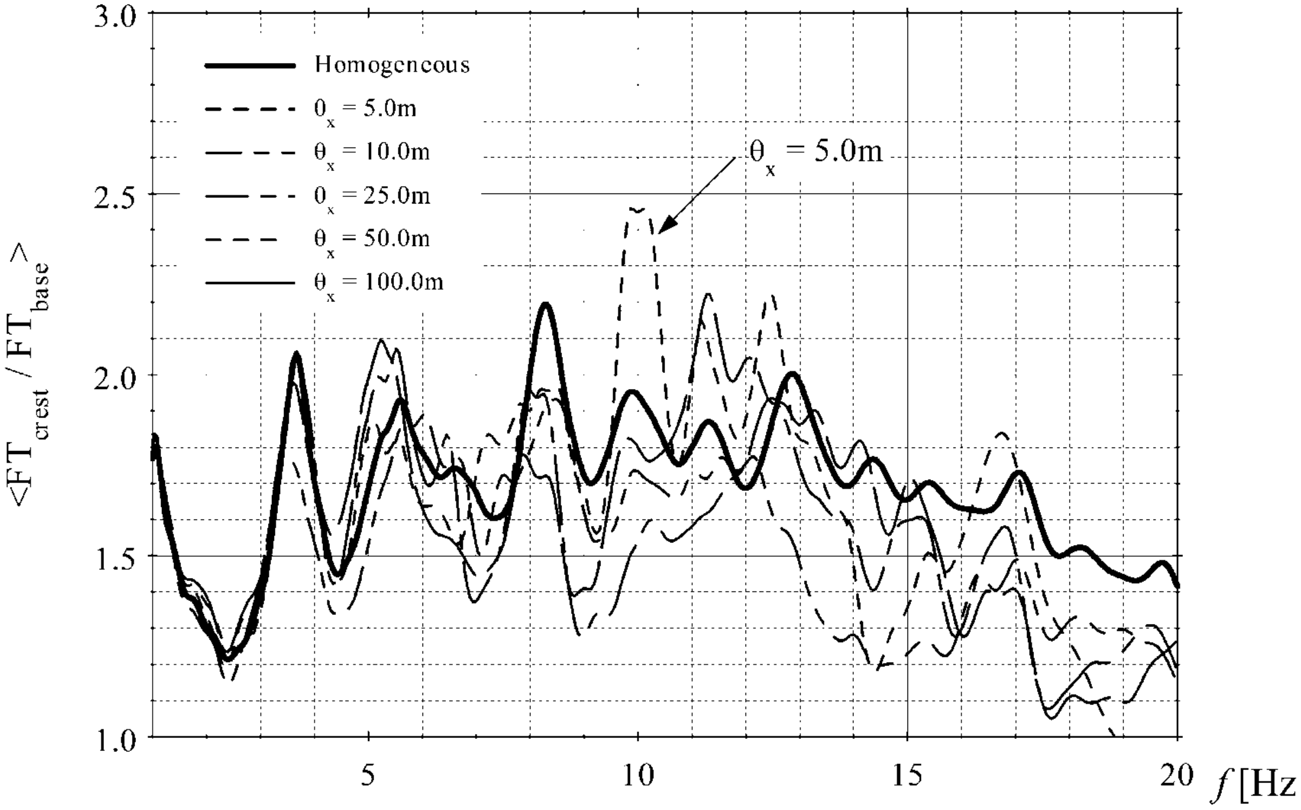

Variation of Fourier Amplitude Ratio from crest to base as a function of correlation distance for a non-homogenous layered slope (Assimaki et al. 1999)

Background

- 2D numerical studies mostly under predict amplifications in the field
- 3D simulations are costly to perform
- Effects not accounted for in GMPEs, and not included in building codes
- Design can be un-conservative on ridges

NSF Topo Project (2009 – 2014)

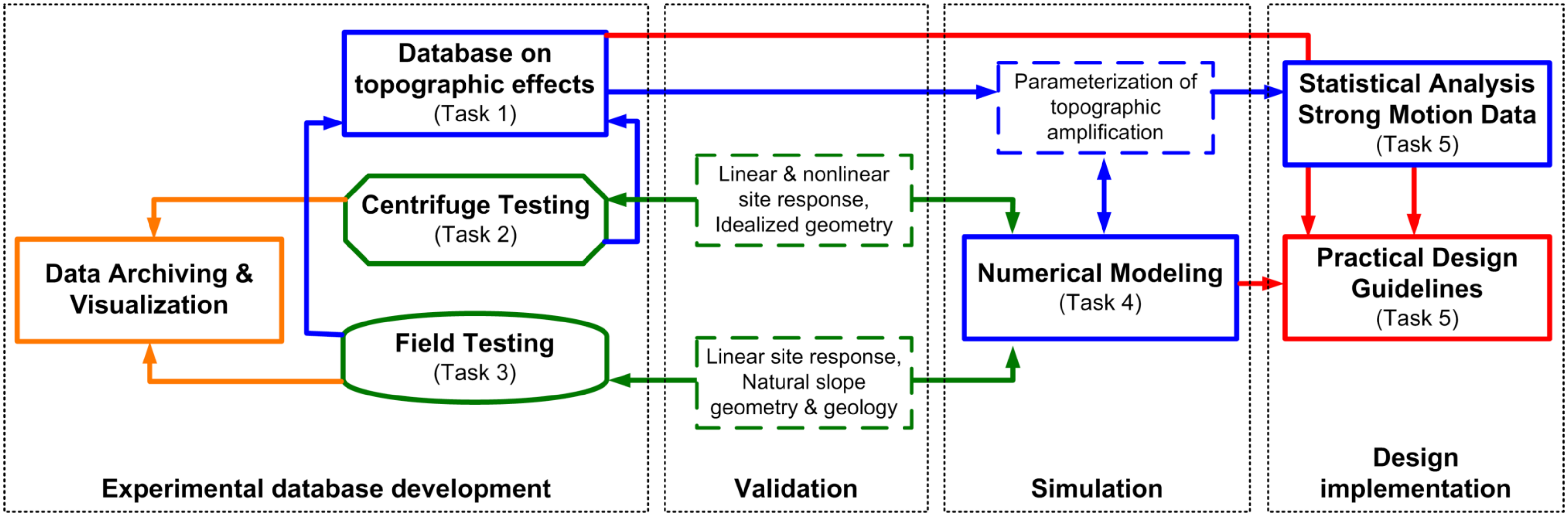

PIs: Dominic Asimaki (CalTech), Brady Cox (U. Texas), Joseph Wartman (U. Washington), Miguel Pando (UNCC), and A. Rodriguez-Marek (VT),

NSF Topo Project: Field Results

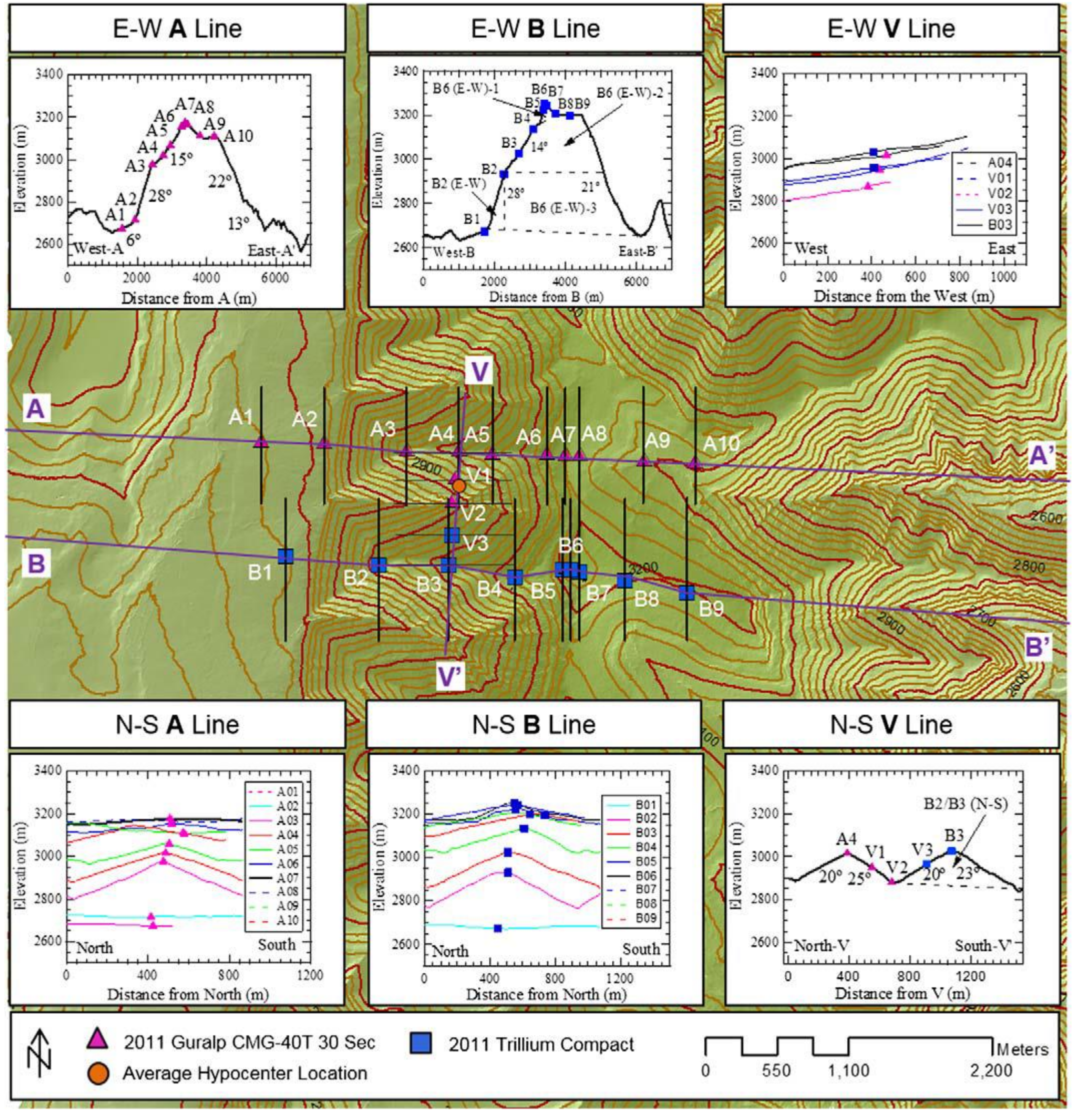

- Recordings of small earthquakes resulting from long-wall mining in Utah
  - Times of earthquakes are known (within days)

Wood, C., Cox, B. (2016). Comparison of Field Data Processing Methods for Evaluation of Topographic Effects. *Earthquake Spectra*, 32 (4) 2127-2147.

Wood, C., Cox, B. (2015). Experimental Dataset of Mining-Induced Seismicity for Studies of Full-Scale Topographic Effects. *Earthquake Spectra*, 31(1), 541-564.

NSF Topo Project: Field Results

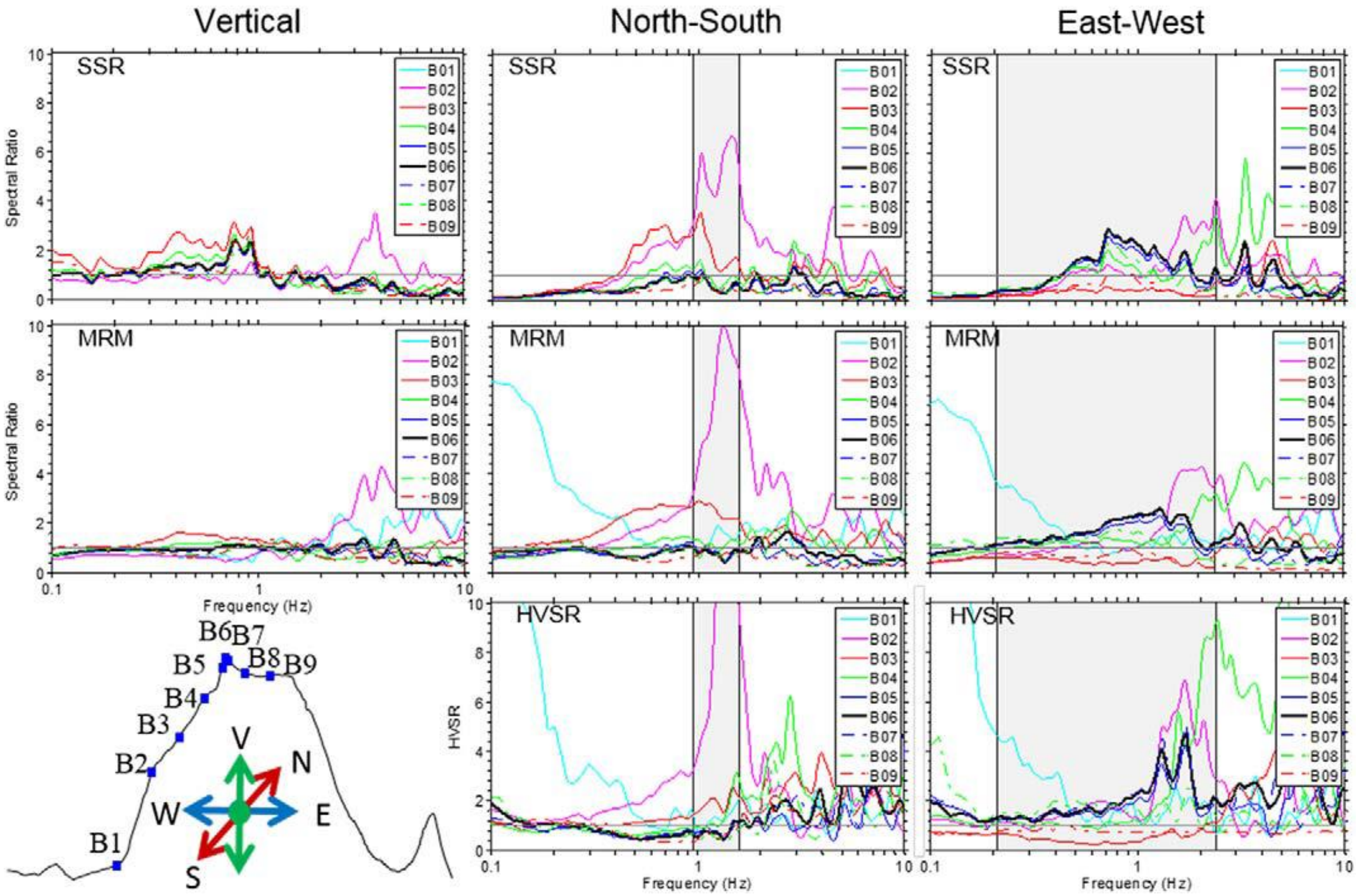

- Results show variability in amplification along the slope
- Amplifications are strongly frequency-dependent

NSF Topo Project: Centrifuge Tests and Numerical Modeling

VirginiaTech Invent the Future®

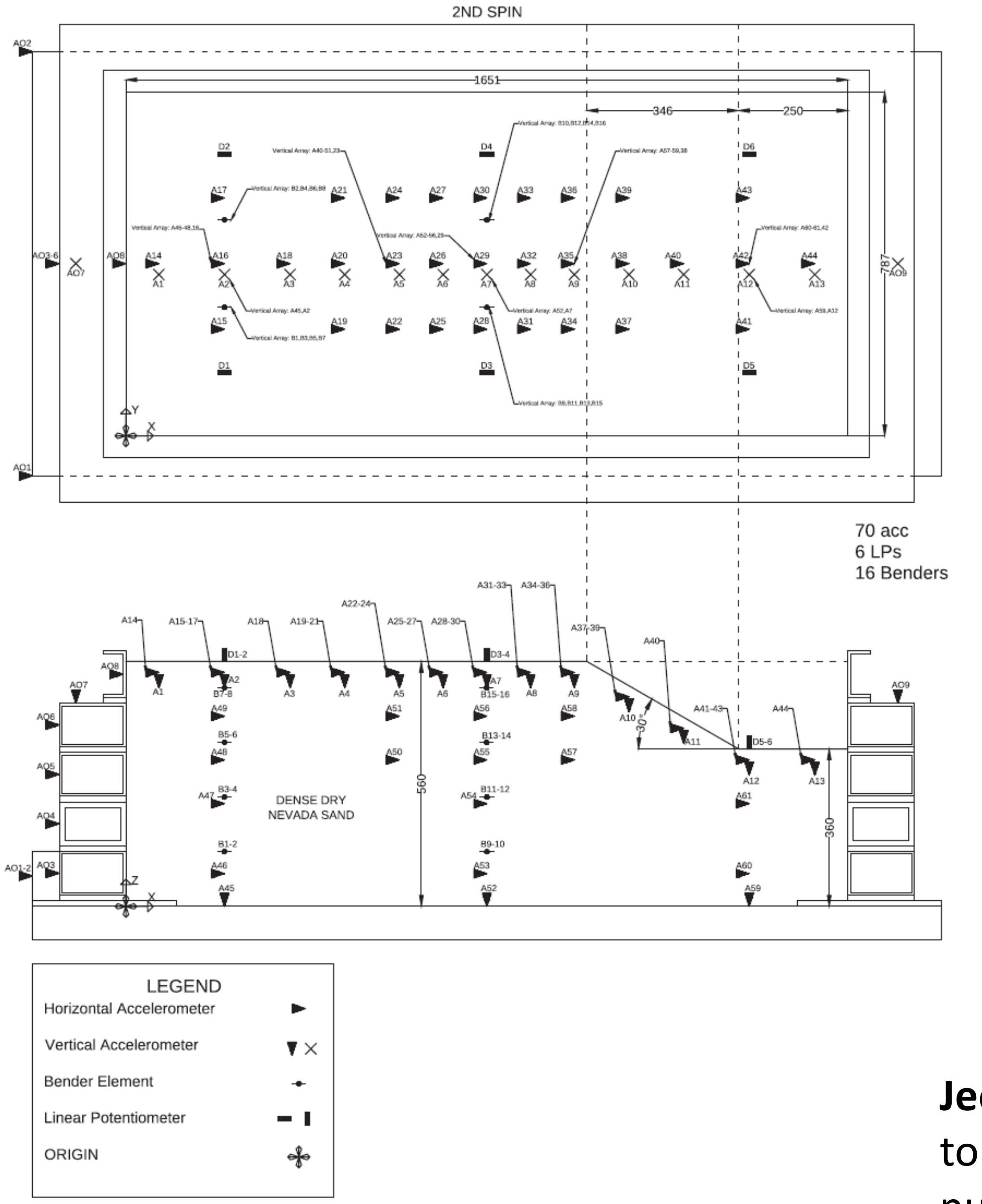

Fig. 6. Sensor deployment plan for the centrifuge model with the 30° slope. Dimensions are in millimeters.

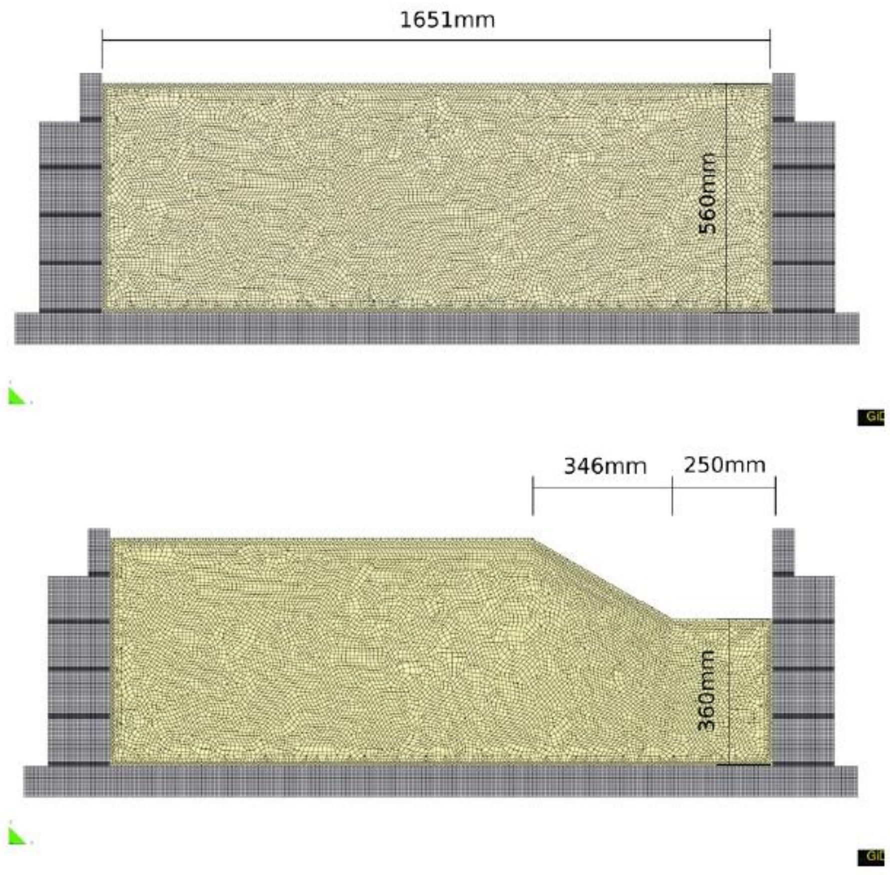

Fig. 2. 2-dimensional finite element mesh of a centrifuge experiment model: a flat ground configuration (top) and a single slope with an angle of 30° (bottom); dimensions shown are in actual model scale.

Jeong, S., Asimaki, D, Dafni, J., and Wartman, J. (2019). "How topography-dependent are topographic effects? Complementary numerical modeling of centrifuge experiments," SDEE 116, 654-667.

NSF Topo Project: Centrifuge Tests and Numerical Modeling

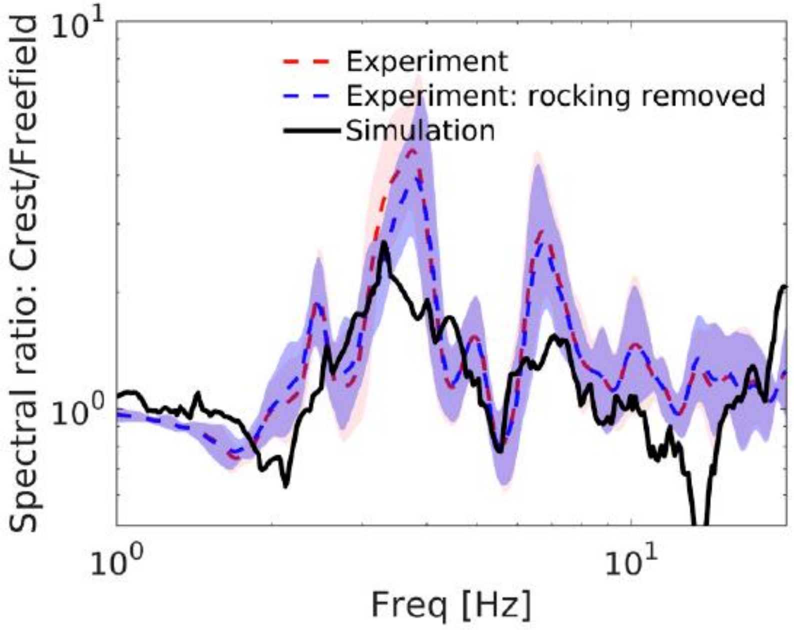

Fig. 16. Effect of the container rocking to the crest-to-freefield spectral ratio at the crest. Spectral ratios are the median of all considered motions.

- Numerical modeling helped identify issues with experimental setup
  - Rocking
  - Effects of container boundaries
- Centrifuge studies validated results from numerical methods
  - Numerical methods can extrapolate results via parametric studies.

NSF Topo Project: Centrifuge Tests and Numerical Modeling

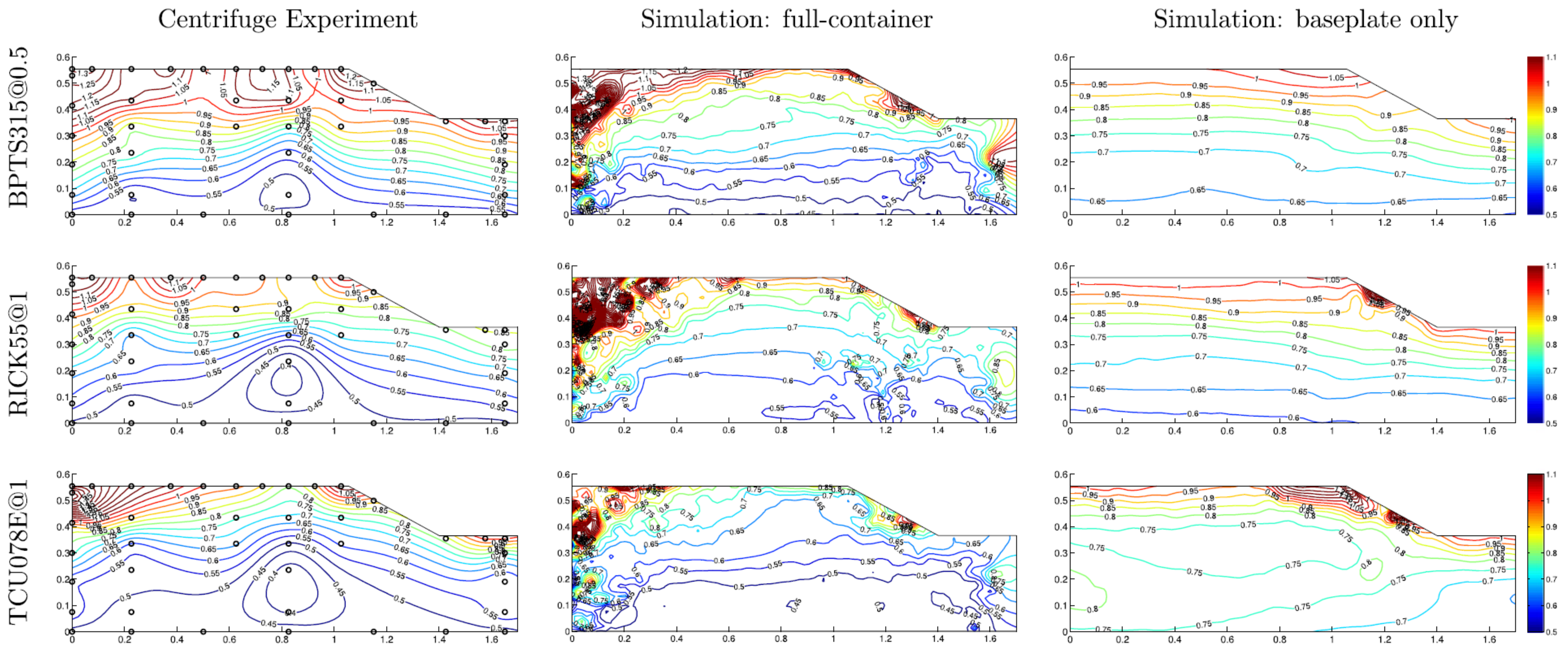

Contours of maximum acceleration

NSF Topo Project (2009 – 2014)

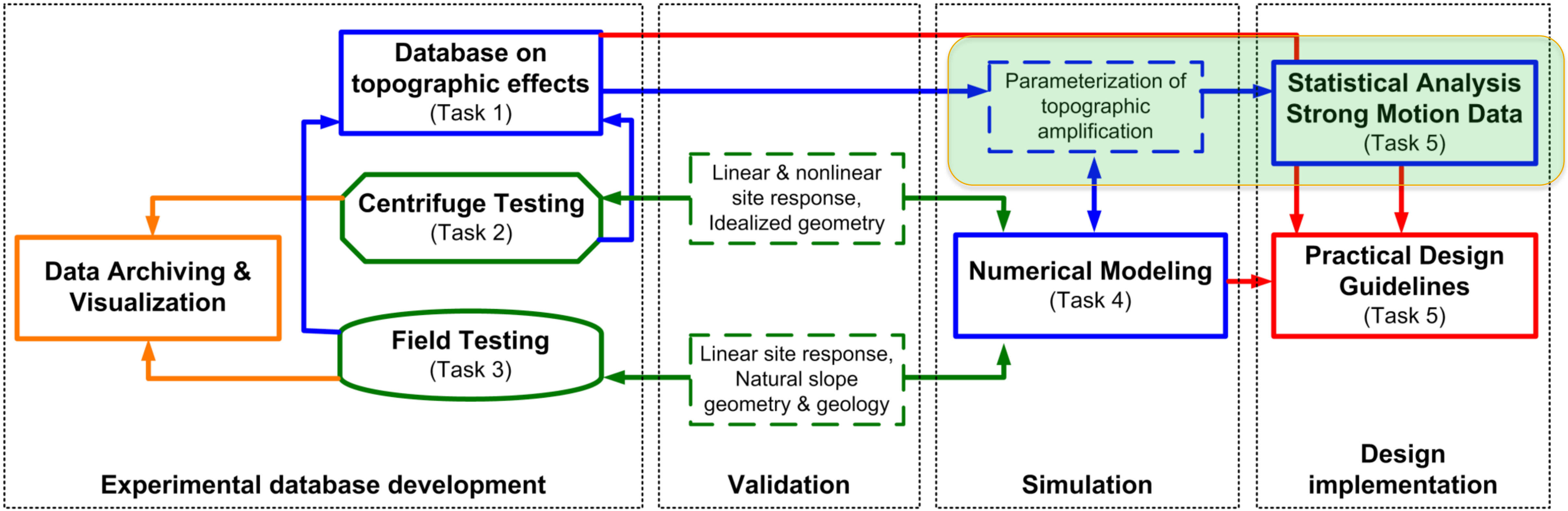

PIs: Dominic Asimaki (CalTech), Brady Cox (U. Texas), Joseph Wartman (U. Washington), Miguel Pando (UNCC), and A. Rodriguez-Marek (VT),

Objective

- Develop empirical models to predict topographic effects through analyses of strong ground motion dataset
  - Predictions represent average behavior with its uncertainty – overcome issues of special variability
  - Easy applicability through GMPEs

Analysis methodology

- Data collection
  - Ground Motion Data
    - SMM (California)
    - NGA-West2 (Global)
  - Elevation data
    - All GM stations
- Topographic parameterization
  - Site geometry
  - Simplistic 2-D numerical analyses
- GMPE residual analyses
- Regression

NGA-West2 dataset

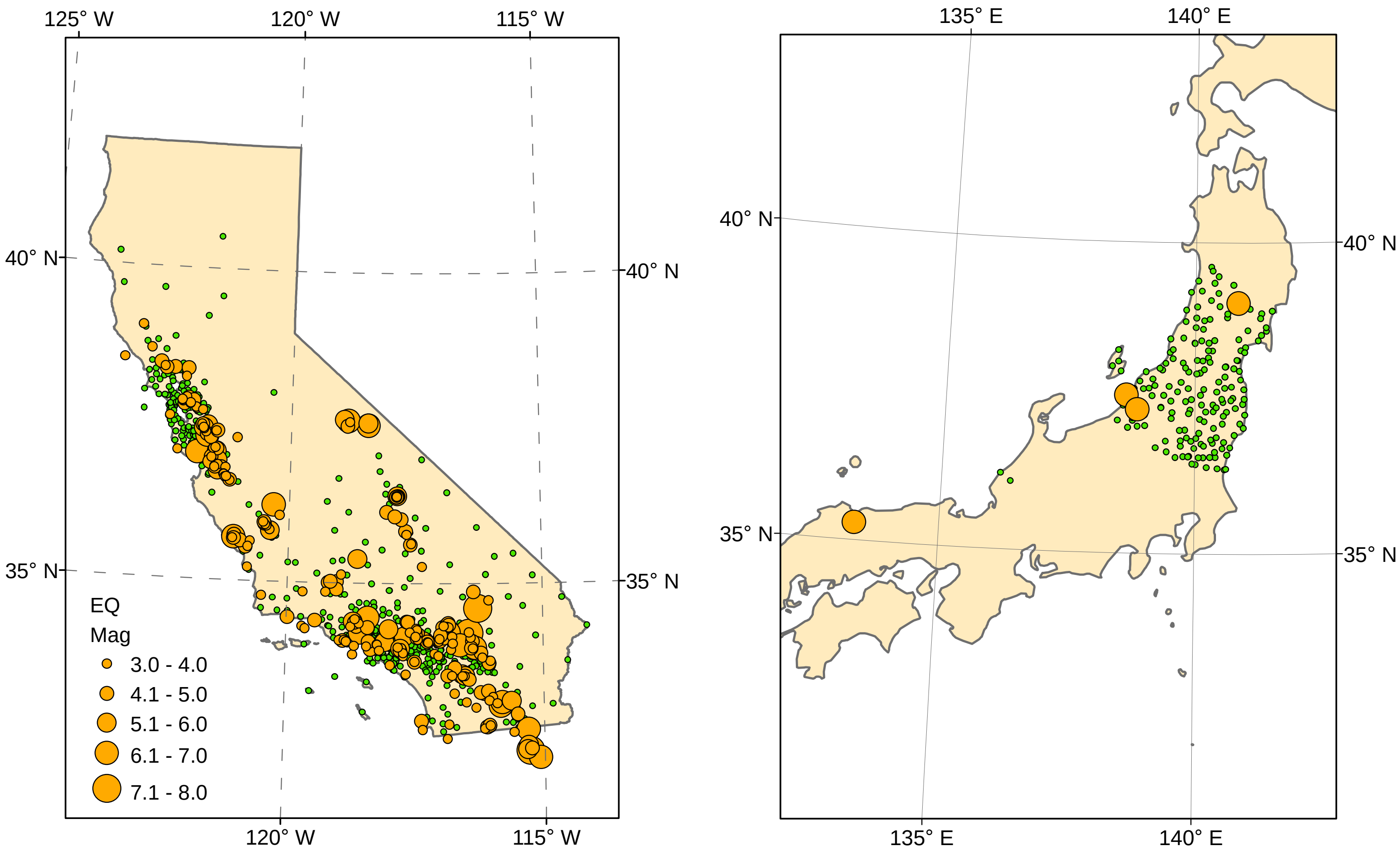

PARAMETERIZATION:
TERRAIN BASED AND NUMERICAL-BASED

Topo parameter: Terrain Based

S_d

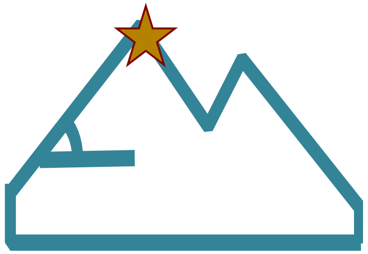

Smoothed slope

Quantifies steepness of a point on the surface

C_d

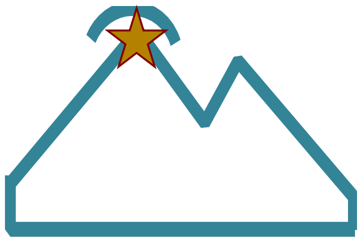

Smoothed curvature

Quantifies convexity or concavity of a point on the surface

Topo parameter: Terrain Based

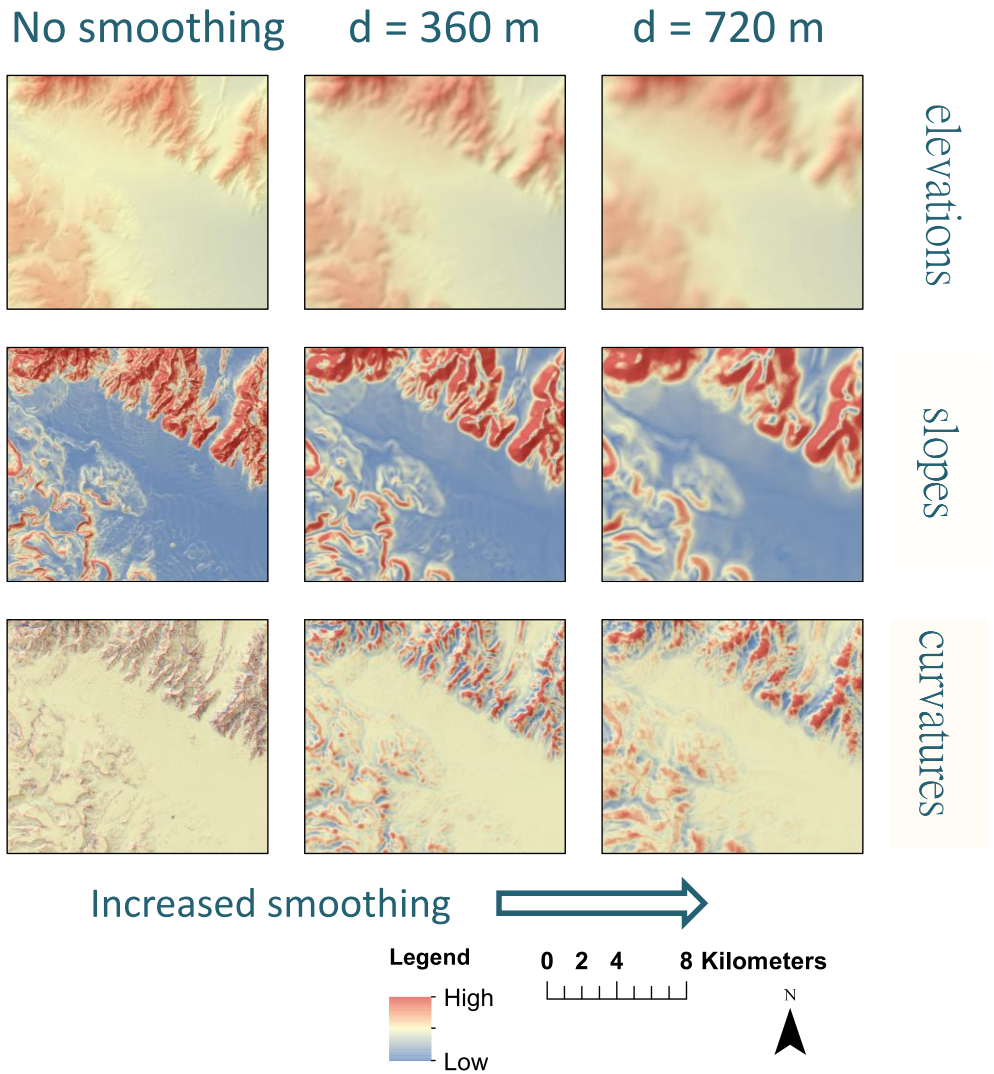

Topo parameter: Terrain Based

H_d

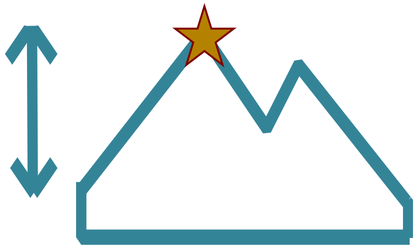

Relative elevation

Quantifies relative height of a point on the surface from its surrounding

S_d

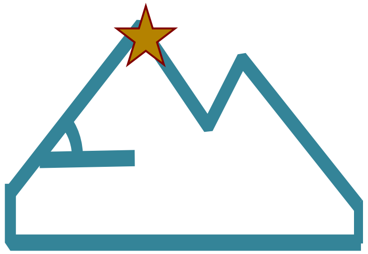

Smoothed slope

Quantifies steepness of a point on the surface

C_d

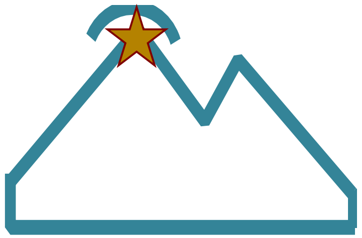

Smoothed curvature

Quantifies convexity or concavity of a point on the surface

Topographic Parameterization: Mean Elevation H_d

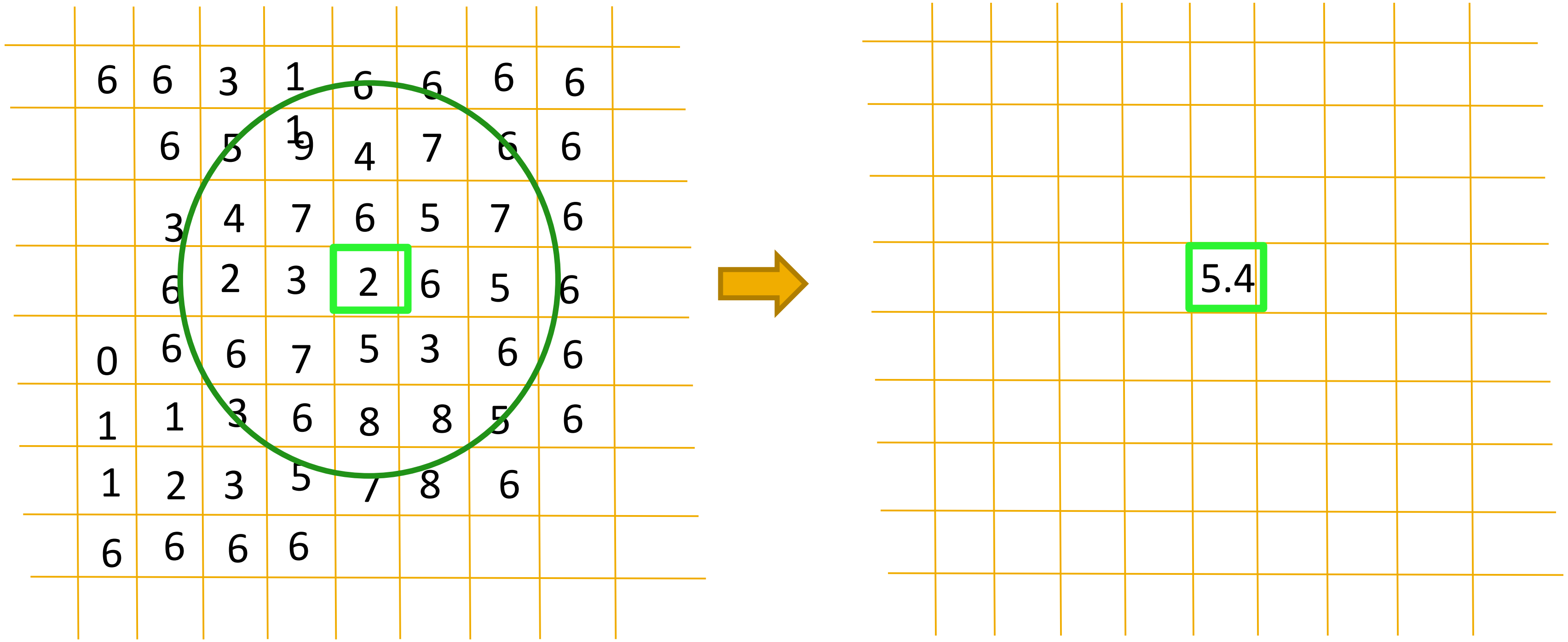

Elevation Raster, h

Mean Elevation Raster, $h_{mean,scale}$

Topographic Parameterization: Mean Elevation H_d

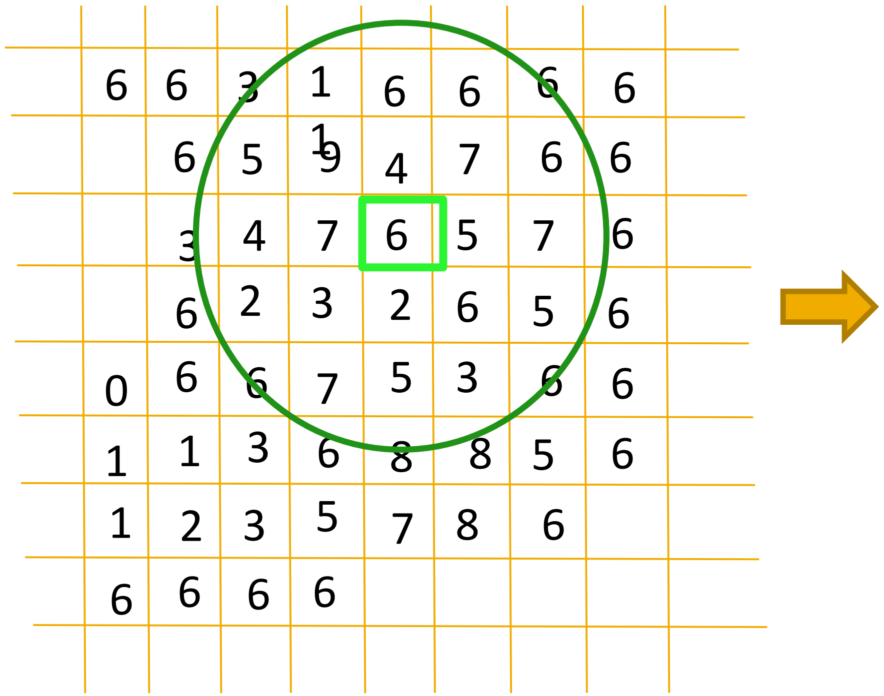

Elevation Raster, h

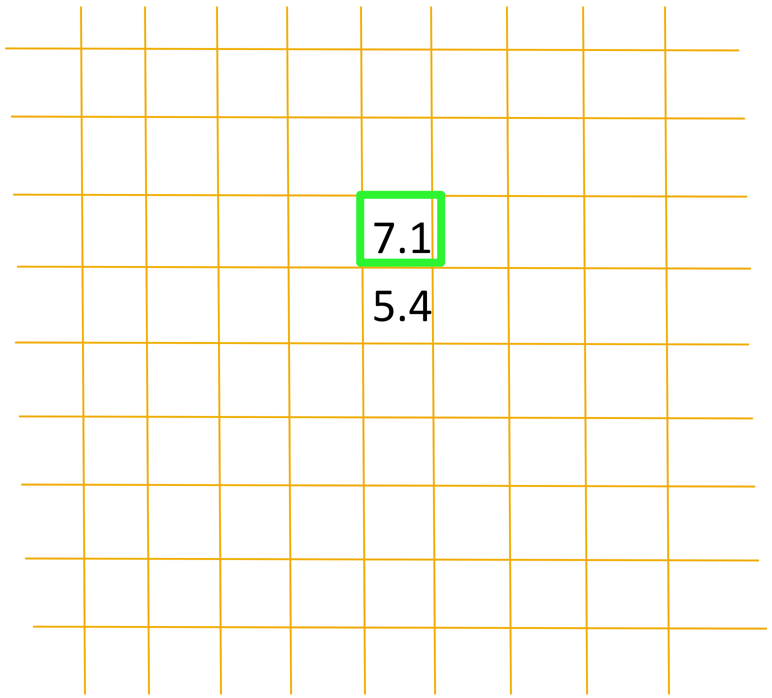

Mean Elevation Raster, $h_{mean,scale}$

Topographic Parameterization: Mean Elevation H_d

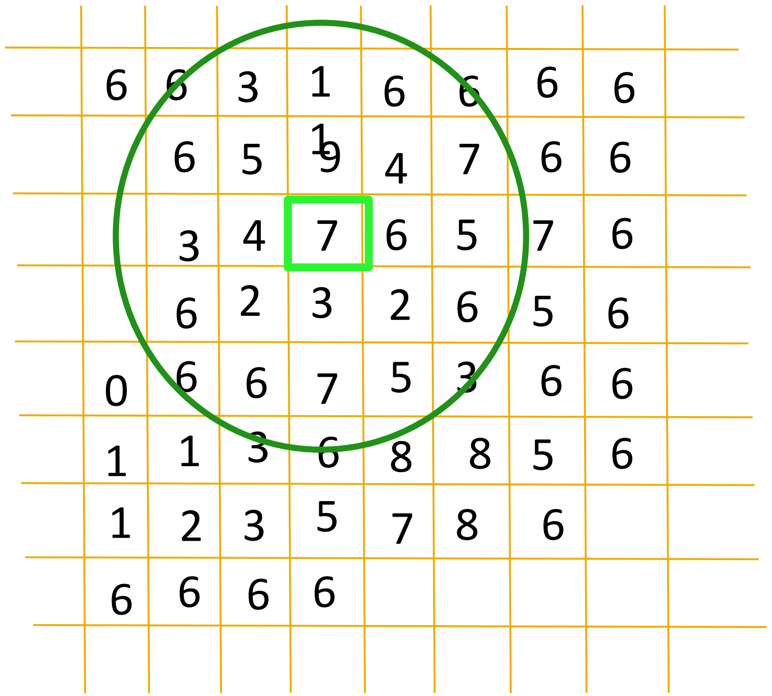

Elevation Raster, h

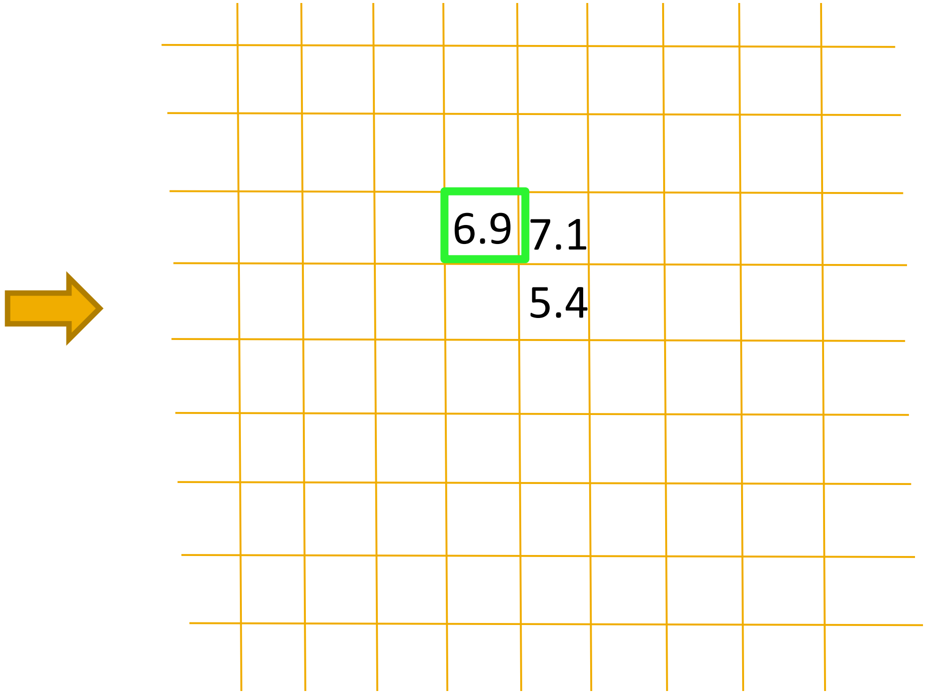

Mean Elevation Raster, $h_{mean,scale}$

Topographic Parameterization: Mean Elevation H_d

6	6	3	1	6	6	6	6
	6	5	19	4	7	6	6
	3	4	7	6	5	7	6
	6	2	3	2	6	5	6
0	6	6	7	5	3	6	6
1	1	3	6	8	8	5	6
1	2	3	5	7	8	6	
6	6	6	6				

Elevation Raster, h

3.1	4.3	5.9	3.1	6.3	4.3	5.9	3.1
6.3	1.8	2.9	7.6	4.7	1.8	2.9	7.6
4.3	6.3	4.7	6.9	7.8	6.3	4.7	4.3
1.8	4.3	5.9	3.1	5.4	4.3	5.9	3.1
1.8	1.3	2.9	7.6	4.7	1.8	2.9	7.6
2.9	1.5	3.4	6.3	4.3	5.5	3.1	6.7
4.3	5.9	3.1	4.3	5.9	3.1	1.8	4.3
1.8	2.9	4.7	1.8	2.9	7.6	4.7	1.8

Mean Elevation Raster, $h_{mean,scale}$

Topographic Parameterization: Mean Elevation H_d

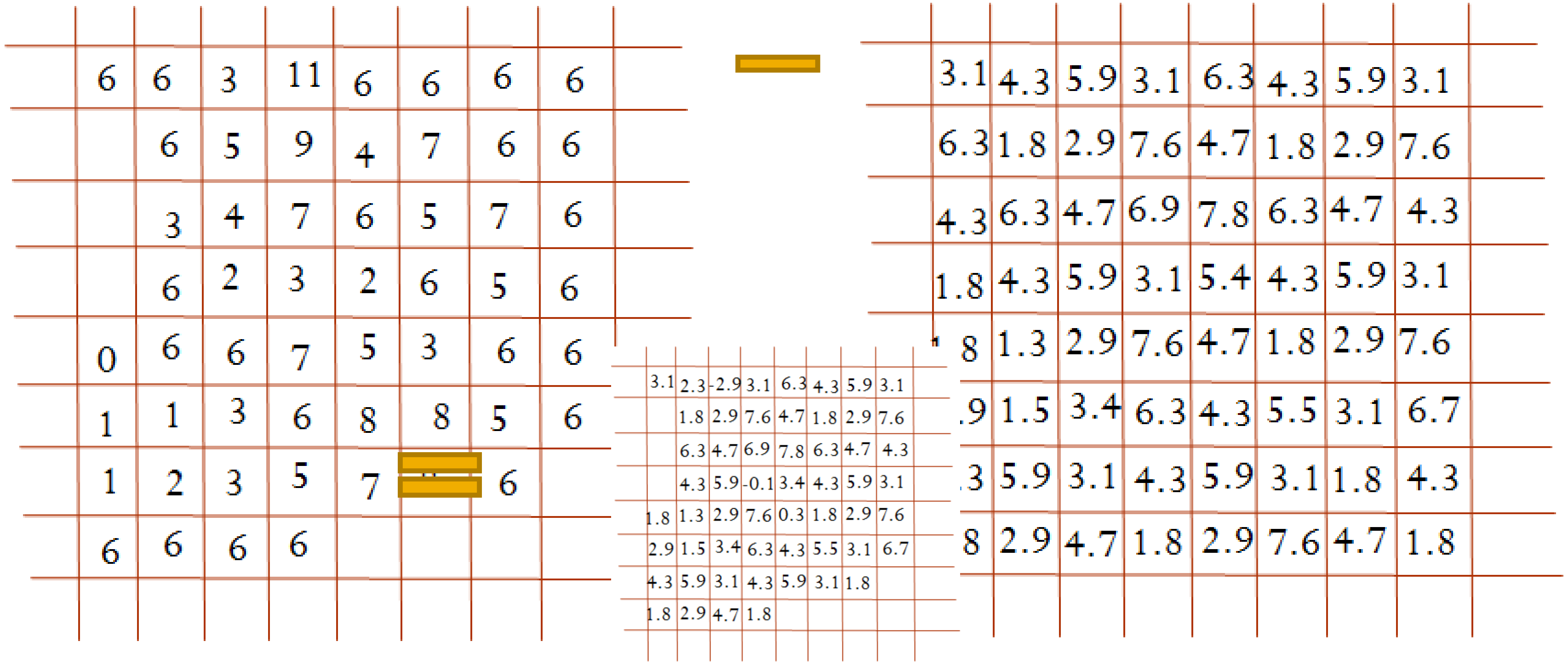

H_{scale}

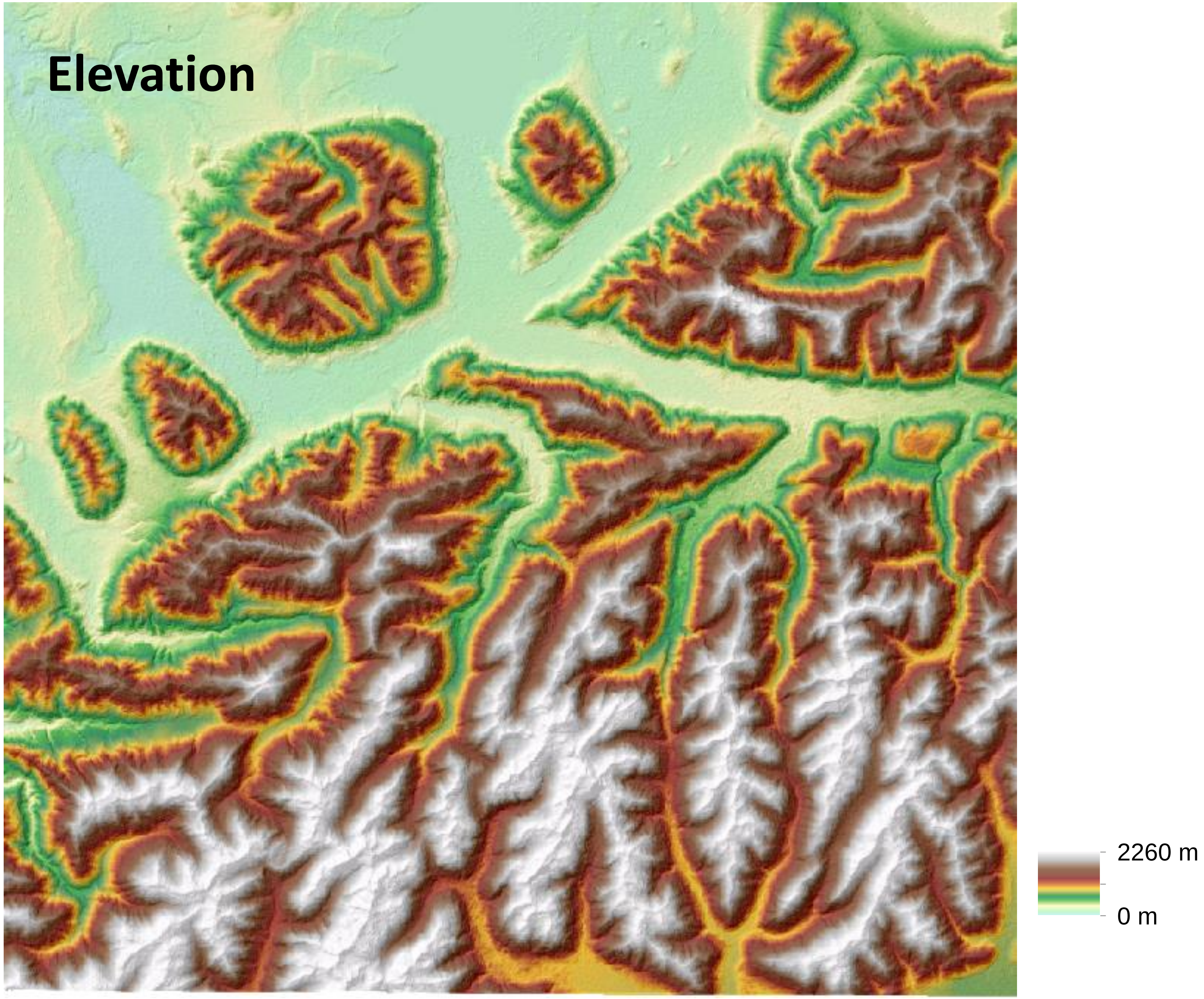
Elevation
2260 m
0 m

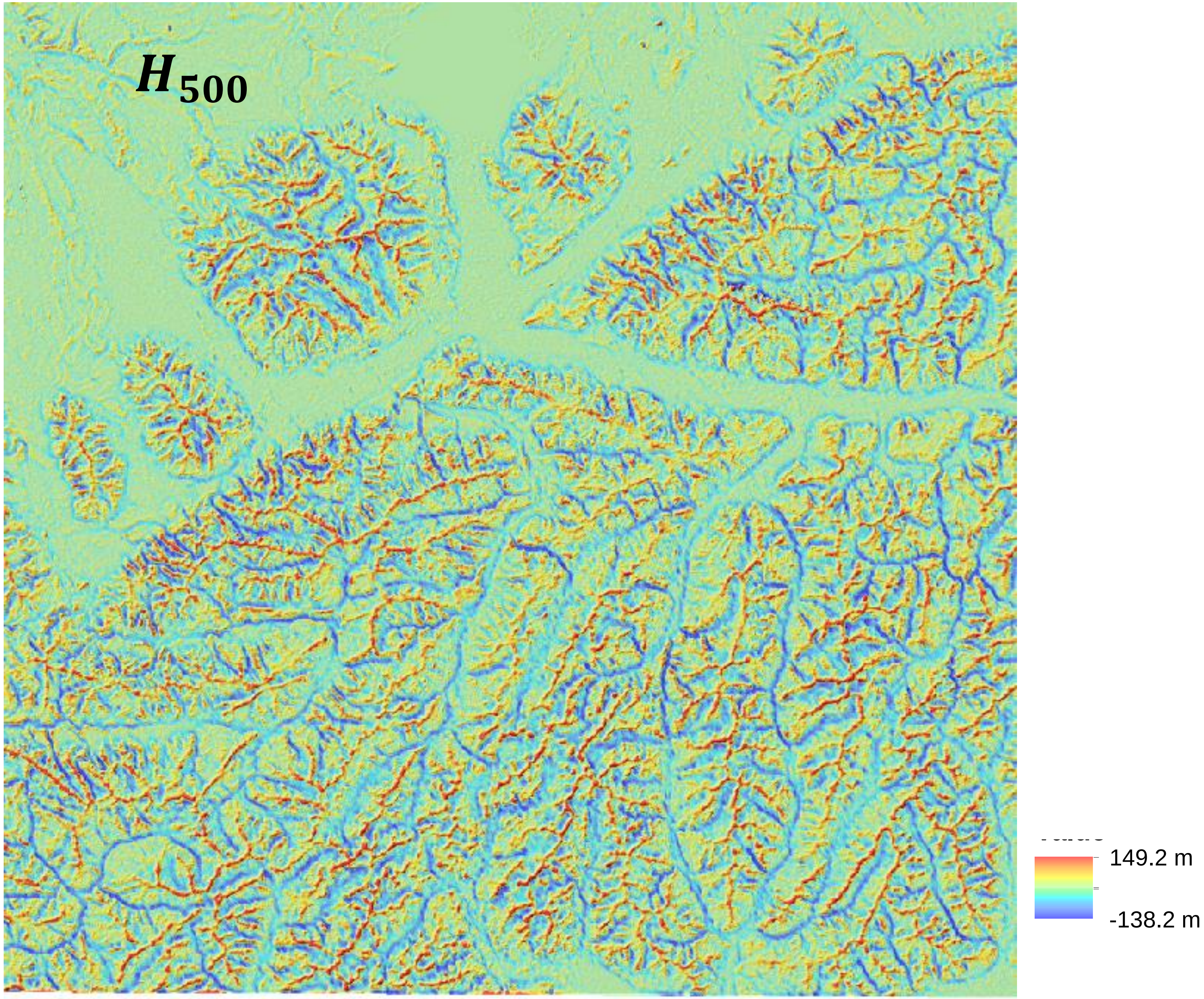
H_{500}
149.2 m
-138.2 m

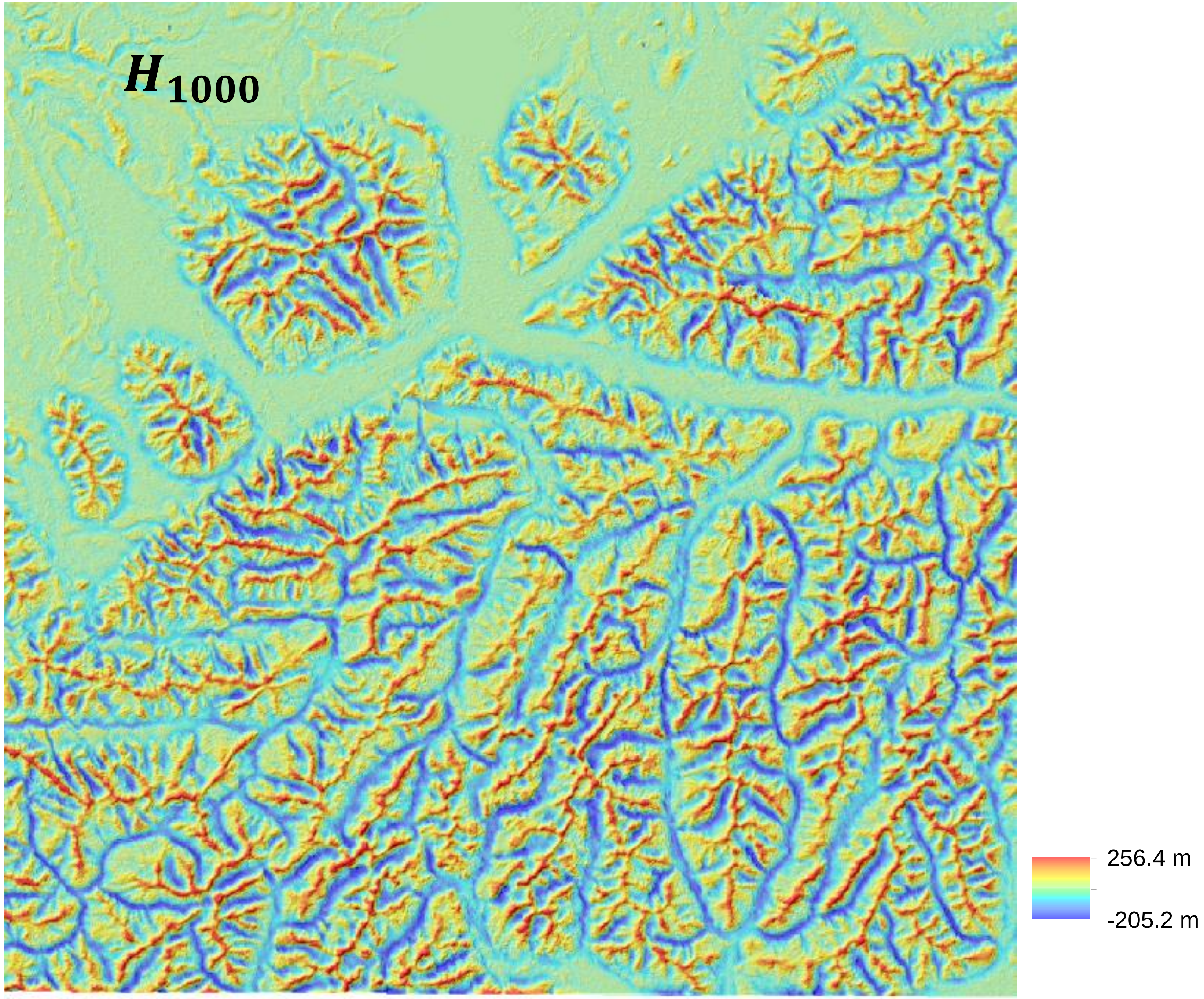
H_{1000}
256.4 m
-205.2 m

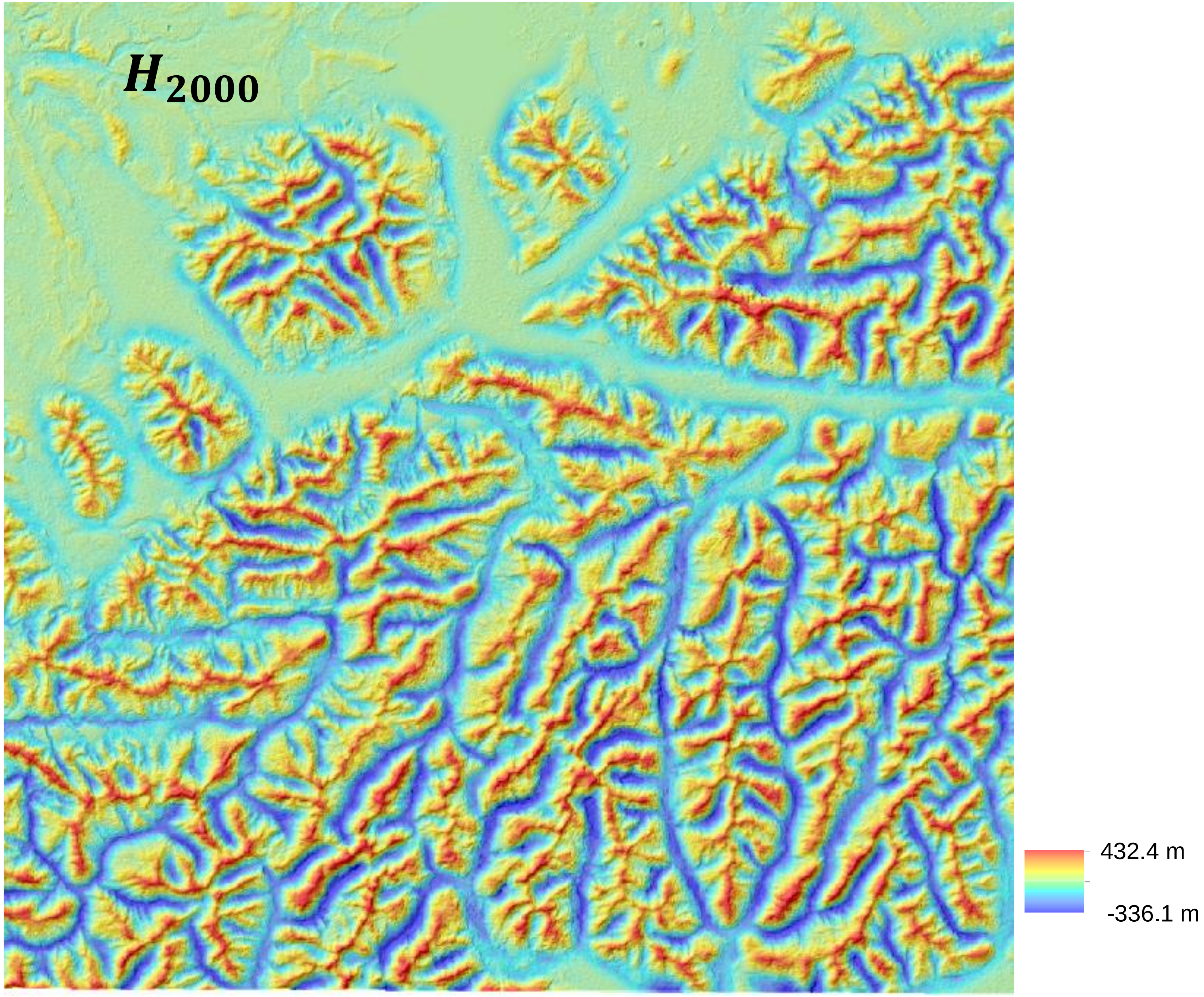
H_{2000}
432.4 m
-336.1 m

Terrain Based Parameterization

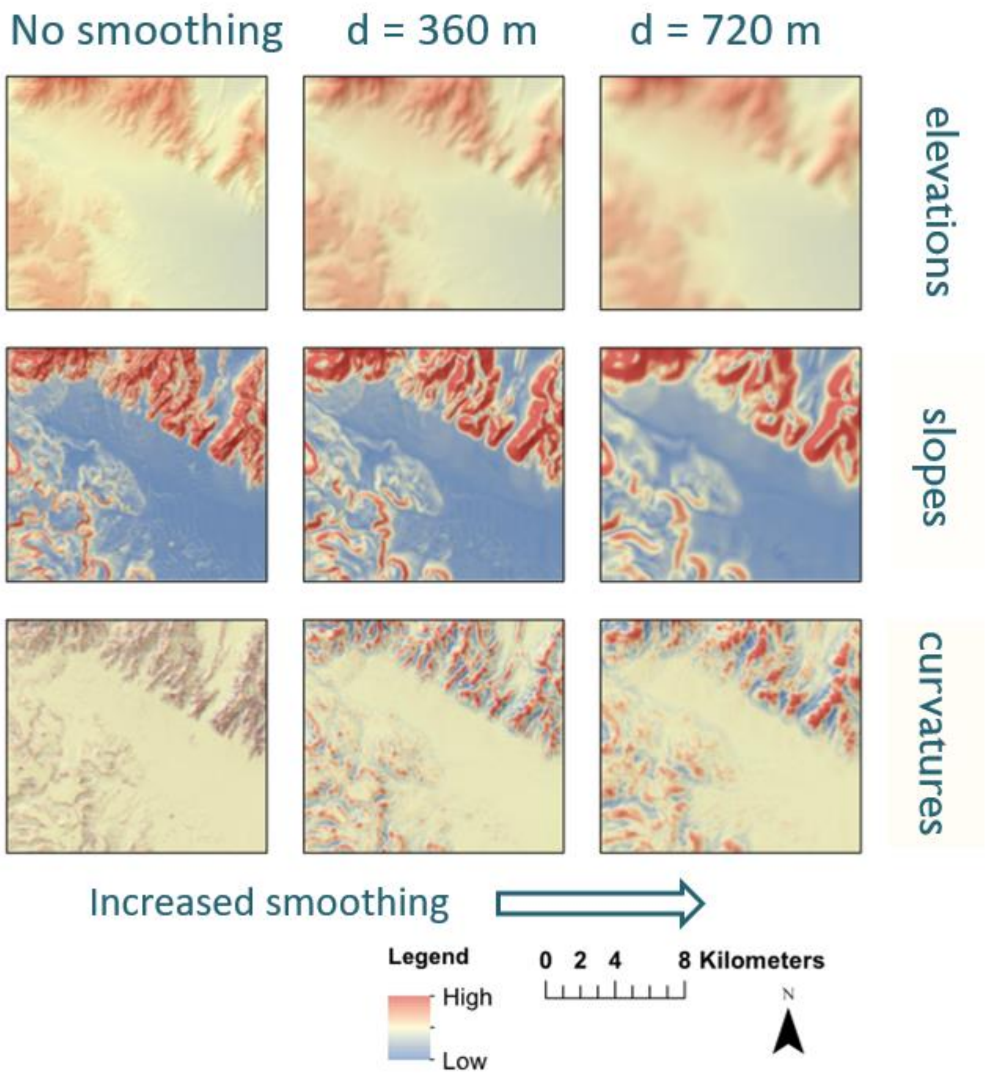

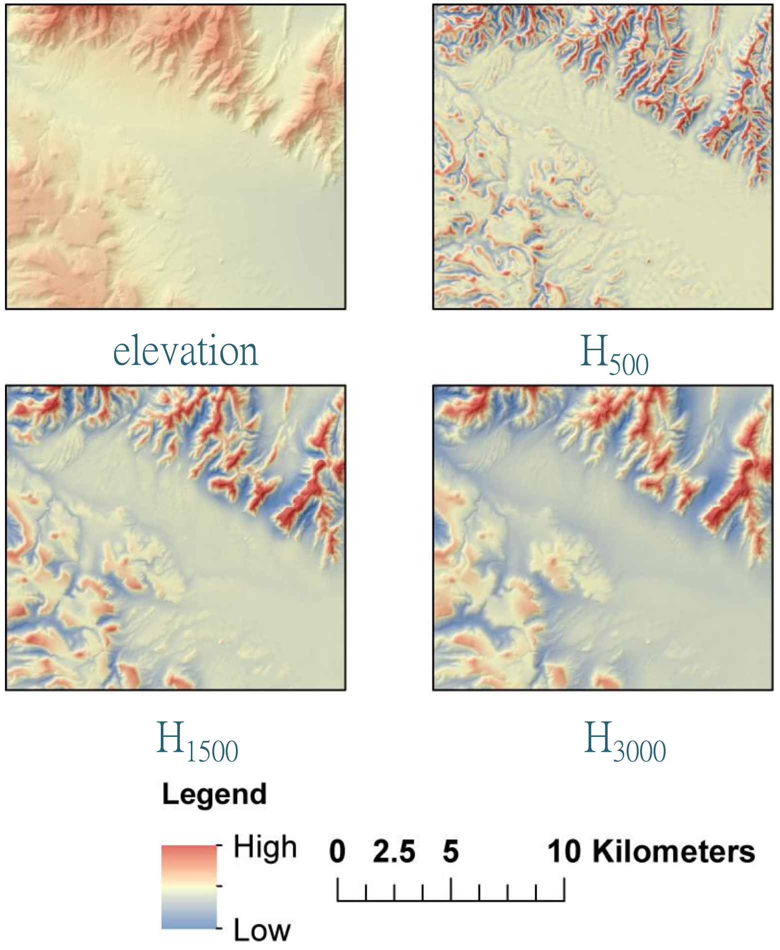

Terrain Based Parameterization

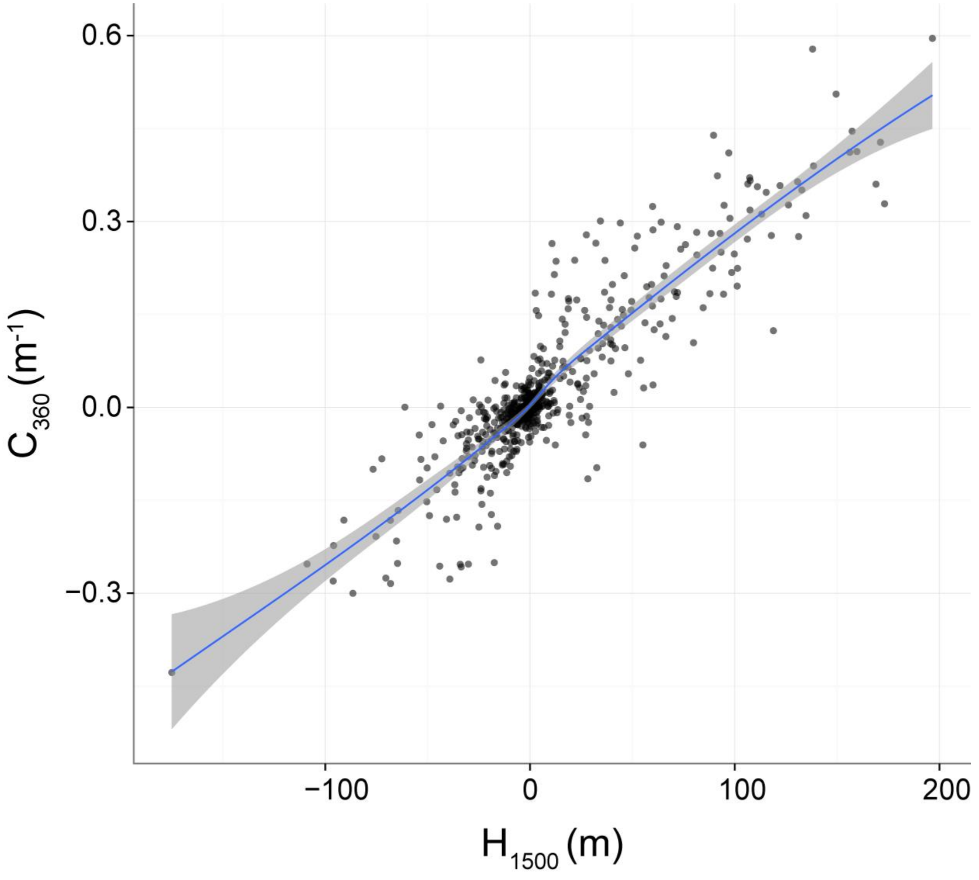

Relative elevation is strongly correlated to smoothed curvature

VirginiaTech
Invent the Future®

Terrain Based Parameterization

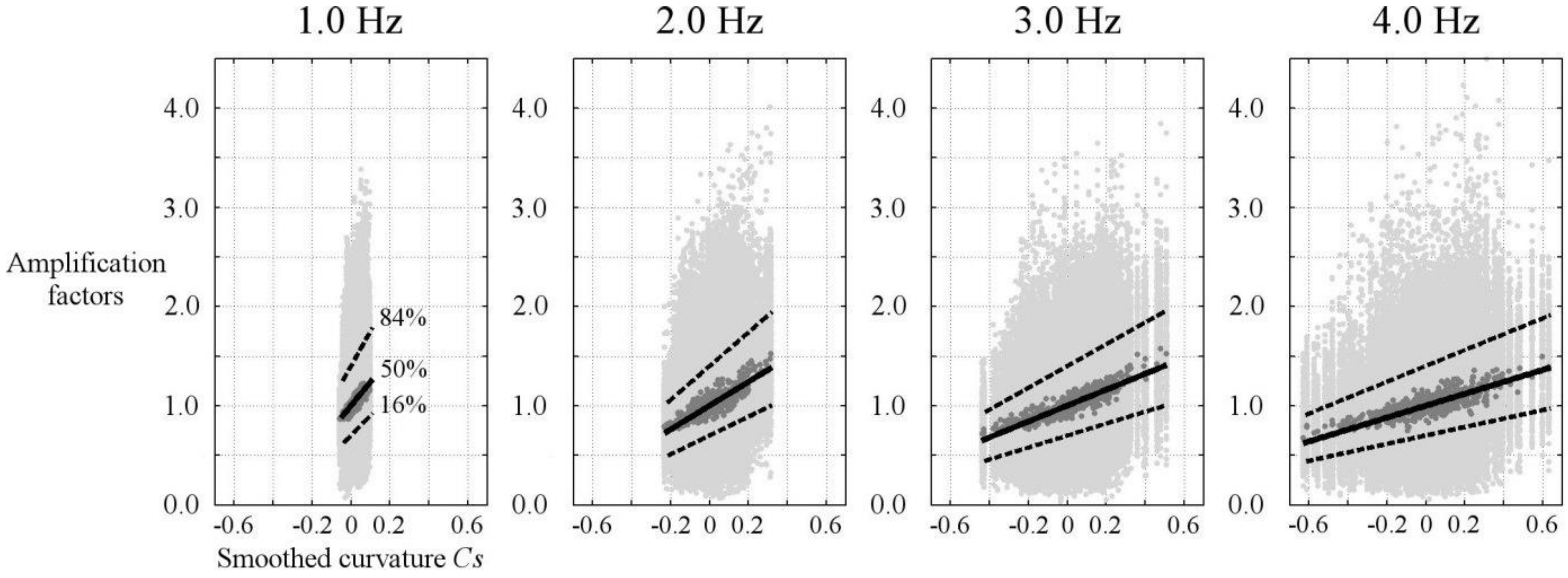

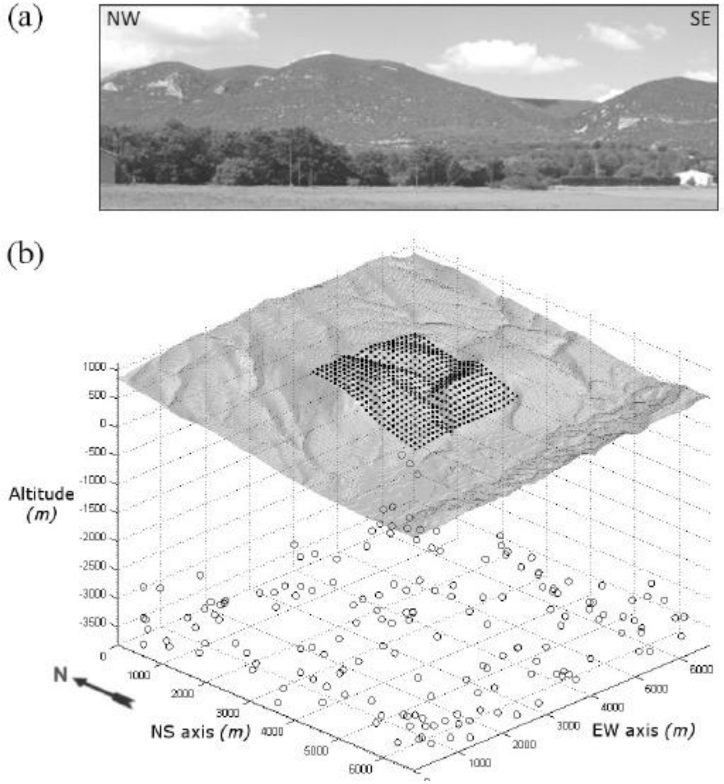

Amplification factors versus smoothed curvature from an artificial ground motion dataset generated using 3D finite diference modeling using measured surface topography in a site in France (right side) for 200 double-couple sources.

From Maufroy et al. (2014

The highest linear correlation is reached when the curvature is smoothed over a characteristic length equal to the S-wavelength divided by two

- **Amplification is caused by topographic features whose horizontal dimensions are similar to half of the S-wavelength.**

Topographic parameterization - Numerical

Empirical correlation

$$Amp = \mathrm{f}(Amp_{FD})$$

Predicted spectral amplification ($S_{a,Topo}/S_{a,No\ Topo}$)

FD prediction of a simplified profile

- 2-D cross-sections
- Ignore 3-D effects
- Elastic analysis
- Simplified input motions
- Multiple azimuths

- Not a predictive exercise
- Family of predictive parameters
- Use recorded data to compute empirical correlation

Topographic Parameterization: FD Analysis

What is V_{s30} ?

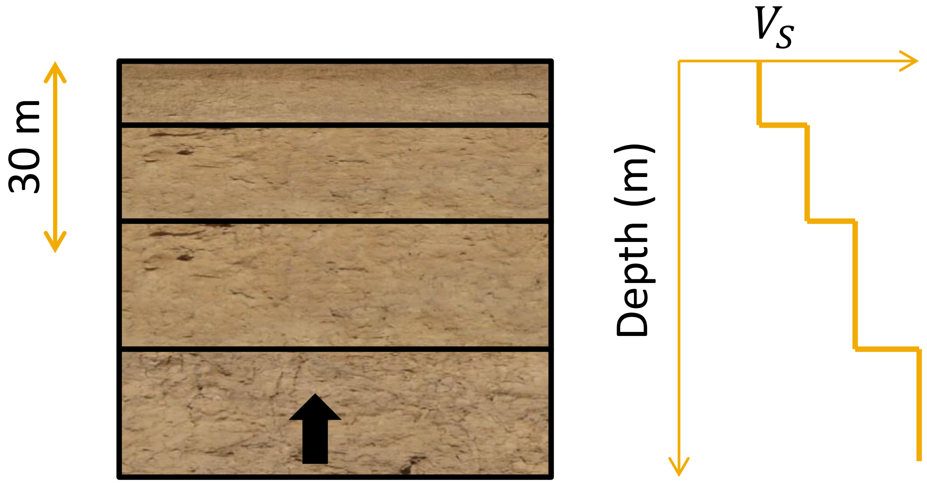

Vertical wave propagation → Travel time in upper 30 m → V_{s30}

Vertical wave propagation

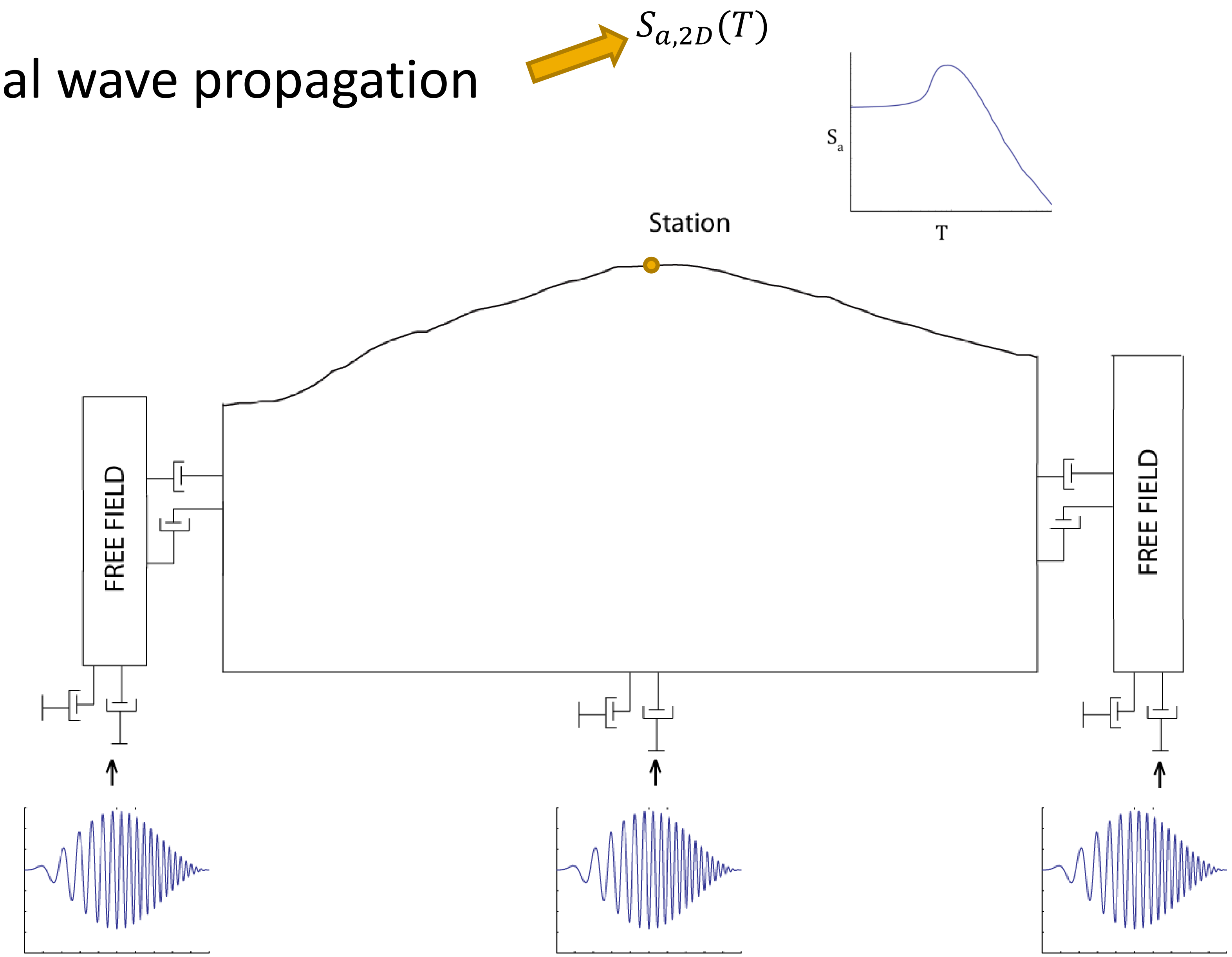

Vertical wave propagation

$S_{a,2D}(T)$

$S_{a,1D}(T)$

$\log(S_{a,2D}/S_{a,1D})$

SAR (T)

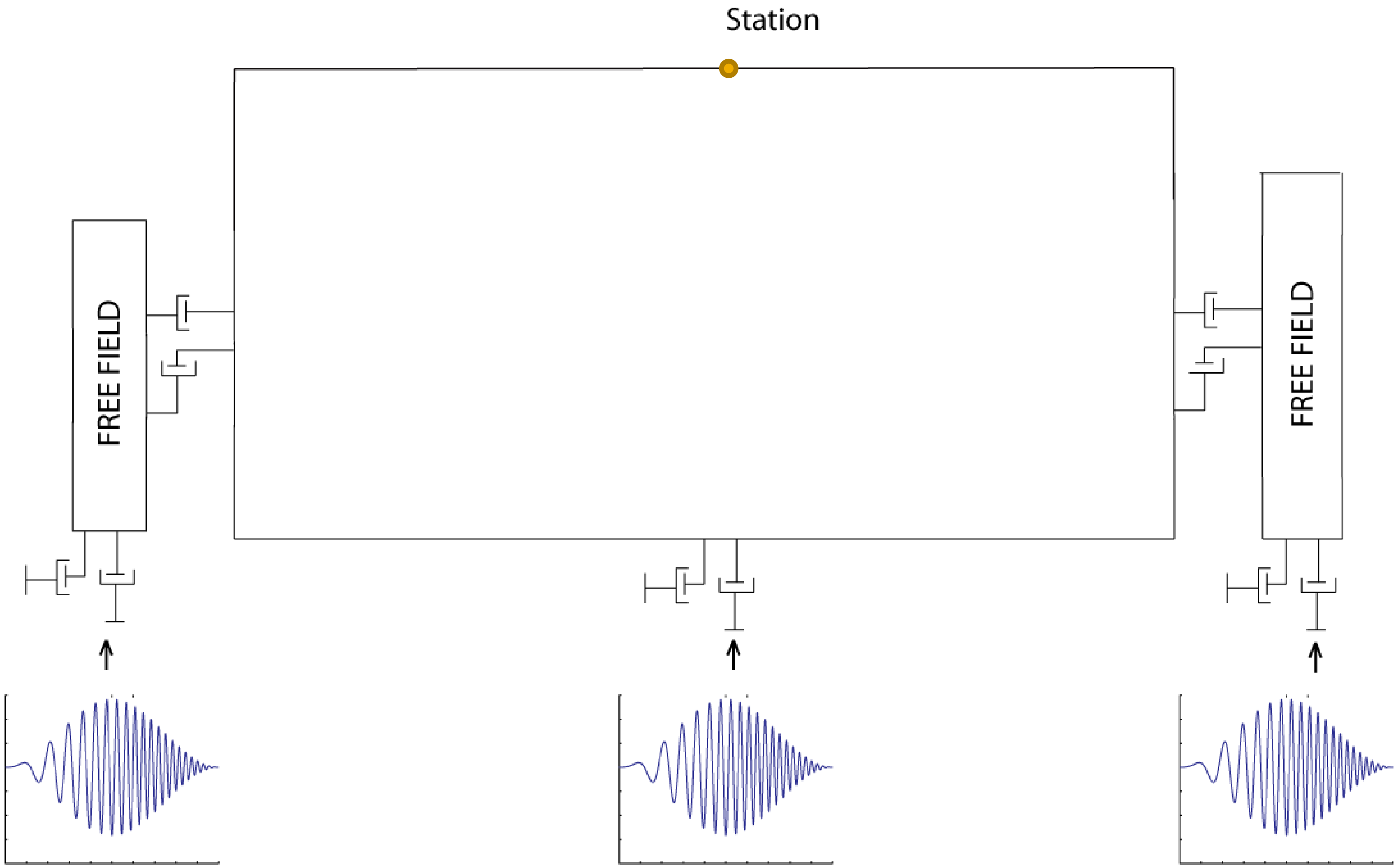

Topo parameter: Numerical

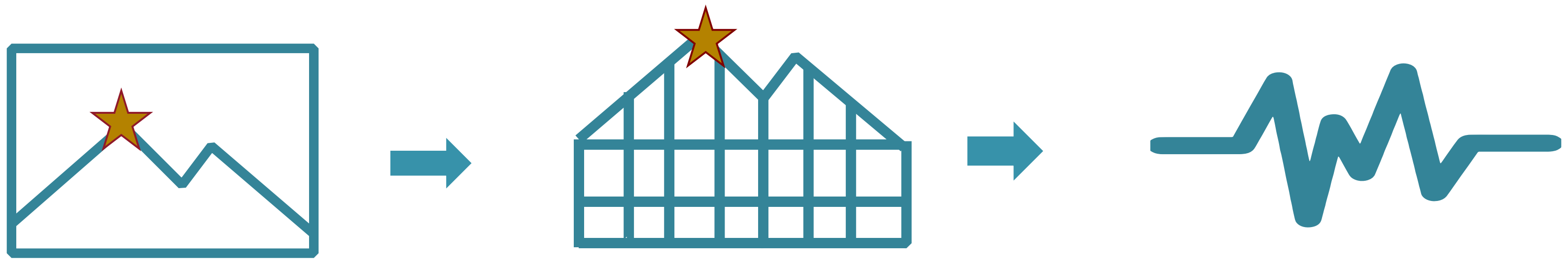

X- sections

FLAC meshes

Output time histories from FLAC

Topo parameter: Numerical

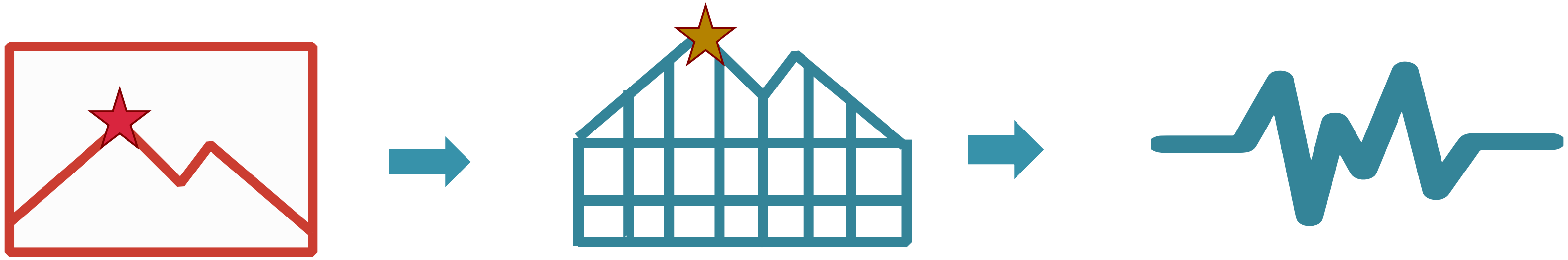

X- sections

FLAC meshes

Output time histories from FLAC

Topo parameter: Numerical

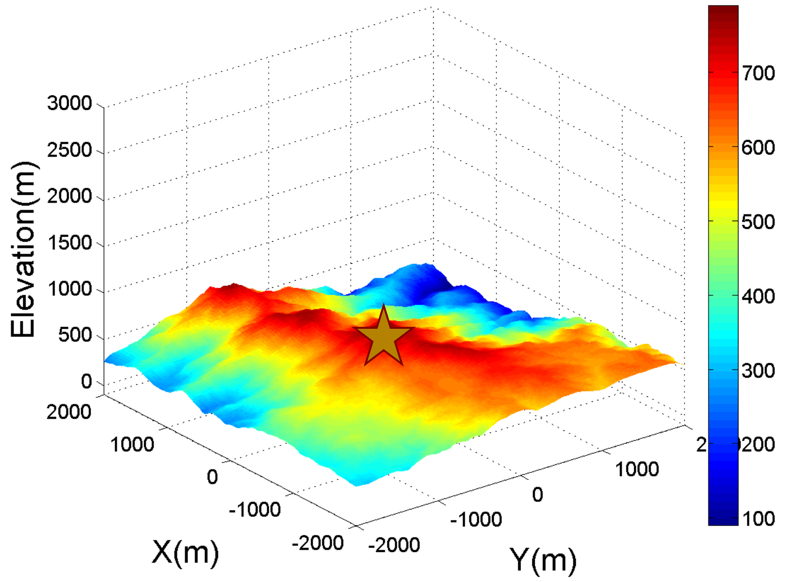

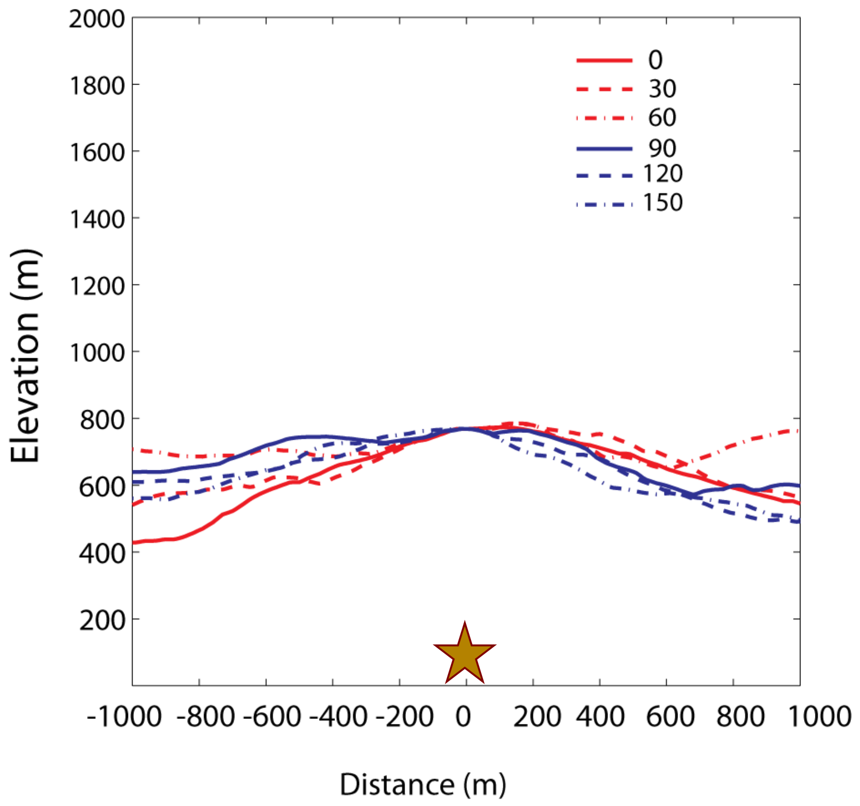

Tamalpais peak station, California

Topo parameter: Numerical

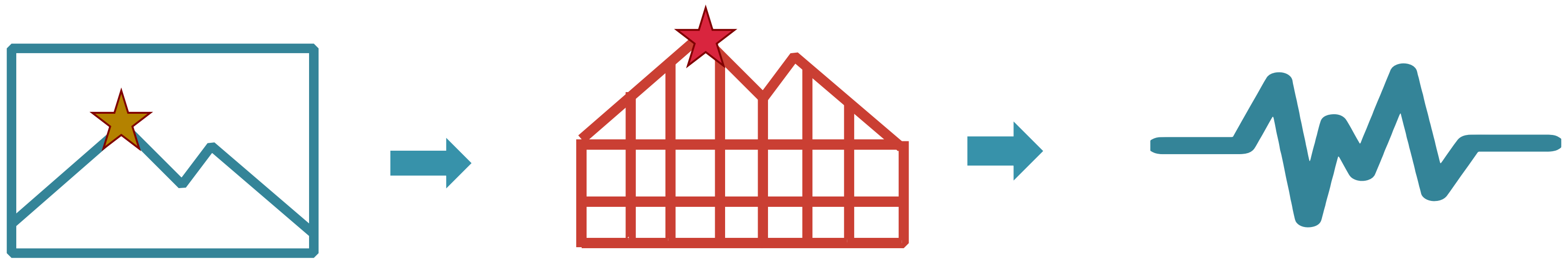

X- sections

FLAC meshes

Output time histories from FLAC

Topo parameter: Numerical

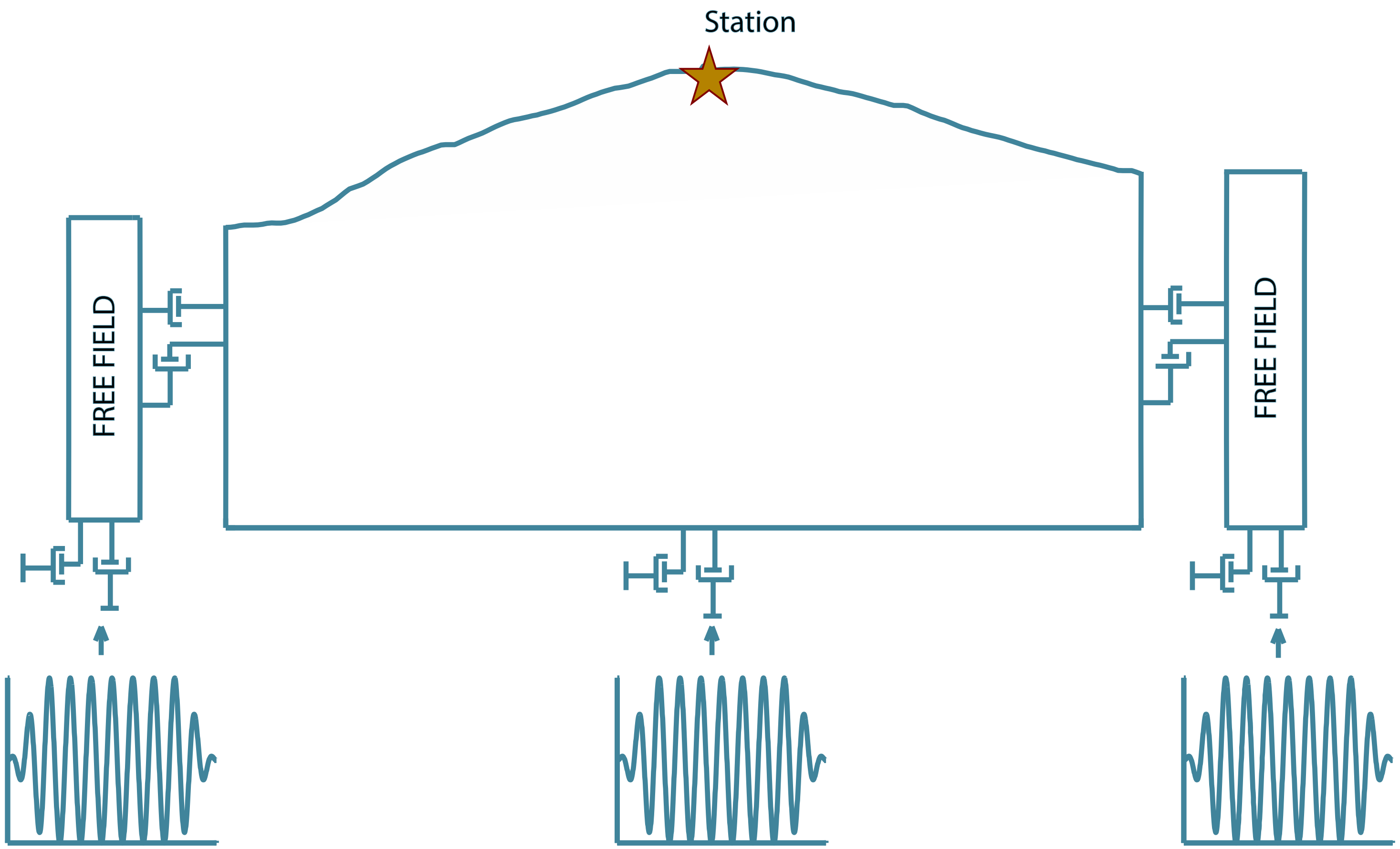

Topo parameter: Numerical

- 2 approaches
  - V_s of 500 m/s for all stations
  - $V_s = V_{s30}$
- 3 periods of input harmonic motion
  - T = 0.5 s, 1 s, and 2 s
- 6 orientations for every GM station
- Total of 23,940 analysis

Topo parameter: Numerical

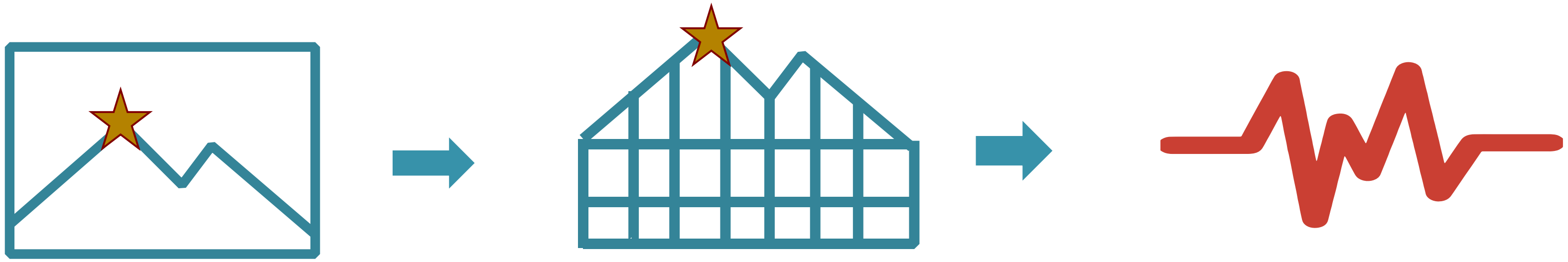

X- sections

FLAC meshes

Output time histories from FLAC

Topo parameter: Numerical

Normalized PGA = PGA $_{2D}$/ PGA $_{1D}$

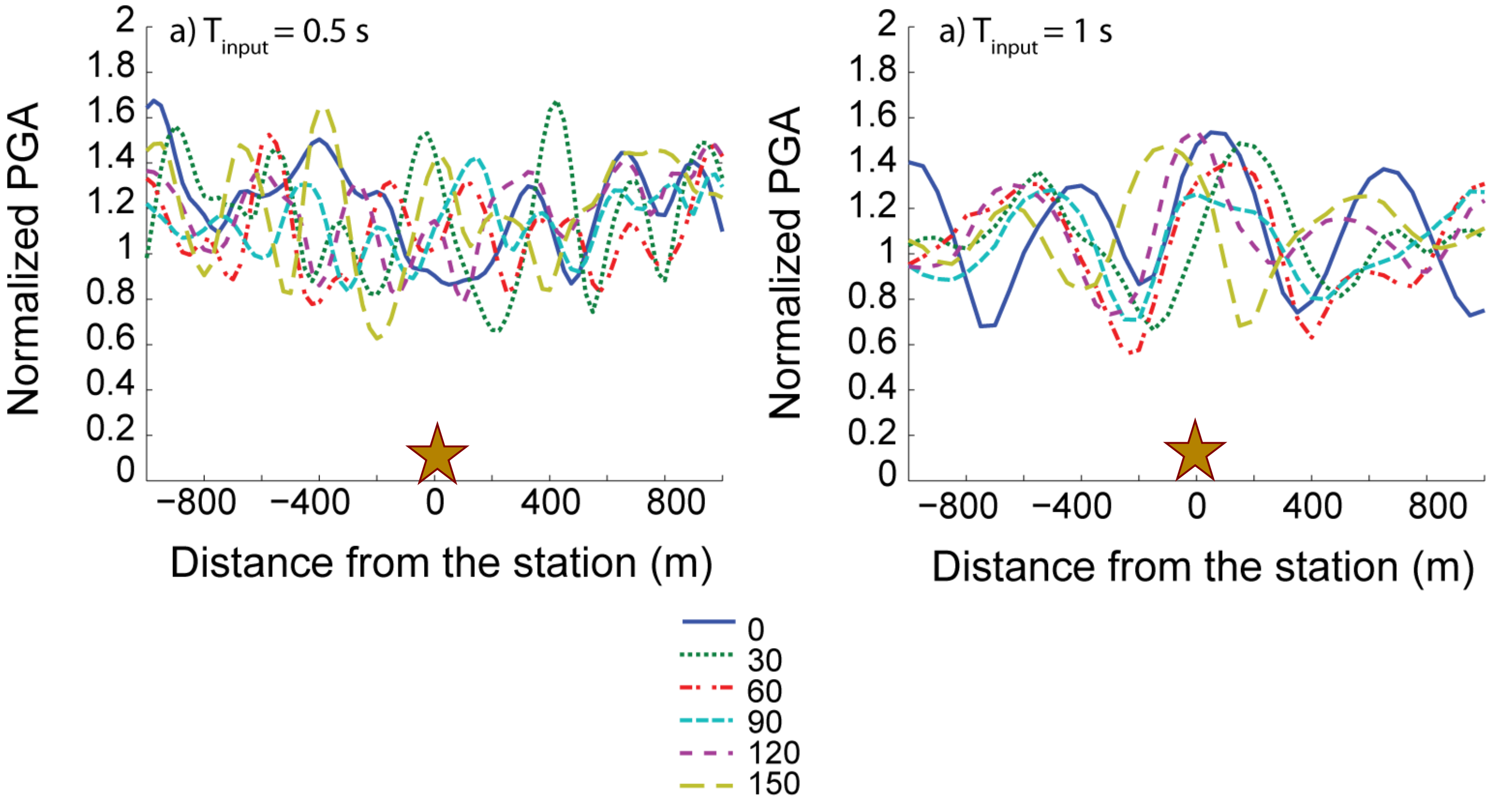

Topo parameter: Numerical

- For a given GM station: use natural log of Normalized PGA (lnAmp) from 6 orientations to develop a family of parameters
  - Maximum, Minimum, Average] Unique to a site
  - Parallel
  - Perpendicular] Unique to a recording

Sta ID	**EQ ID**	**V_{s30} (m/s)**	**S_a (0.01 s)**	**Sa(0.1 s)**	**…**					
1	1	…	…	…						
2	1	…	…	…						
3	2	…	…	…						
4	3	…	…	…						

Sta ID	EQ ID	V_{s30} (m/s)	S_a (0.01 s)	Sa(0.1 s)	…	H_d	S_d	$lnAmp_{max}$	$lnAmp_{avg}$	…
1	1	…	…	…		---	---	---	---	---
2	1	…	…	…		---	---	---	---	---
3	2	…	…	…		---	---	---	---	---
4	3	…	…	…		---	---	---	---	---

RESIDUAL ANALYSES

Residual Partitioning

- GMPE

$$\ln S_a = f(M,R\ldots) + \Delta$$

Median   Residual

Residual Partitioning

- GMPE residuals

$$\Delta_{es} = \delta B_e + \delta W_{es}$$

Event term (↑ δB_e)

δW_{es} ↓

$$\delta S2S_s + \delta WS_{es}$$

Site term (↑ $\delta S2S_s$)

Residual (↑ δWS_{es})

Residual Partitioning

- GMPE residual

$$\Delta_{es} = \delta B_e + \delta S2S_s + \delta WS_{es}$$

  - Site term ($\delta S2S_s$) is the average event-corrected residual at a site
    - The site term contains all the information about the 'repeatable' site effects
    - Our analysis will focus on the site term

Residual Partitioning

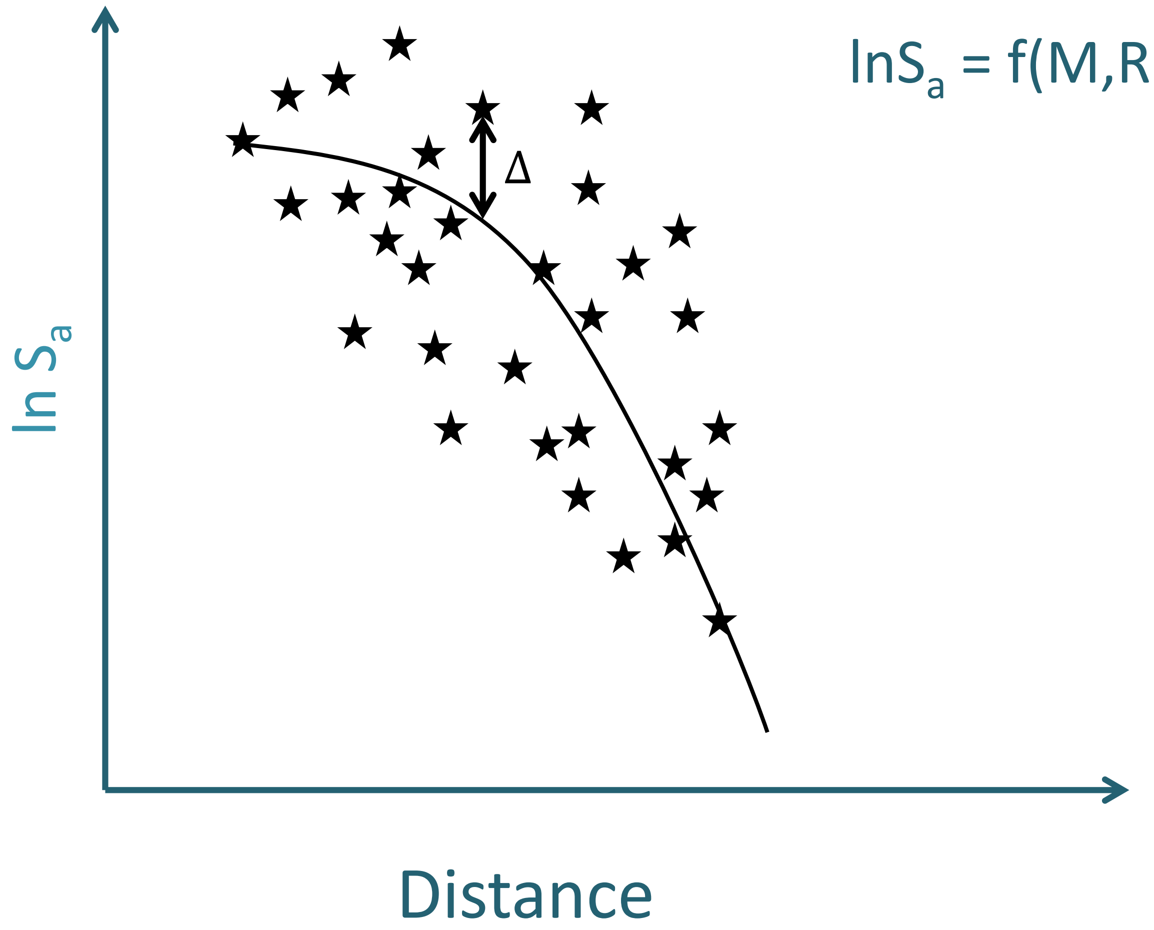

$$\ln S_a = f(M, R\ldots) + \Delta$$

Residual Partitioning

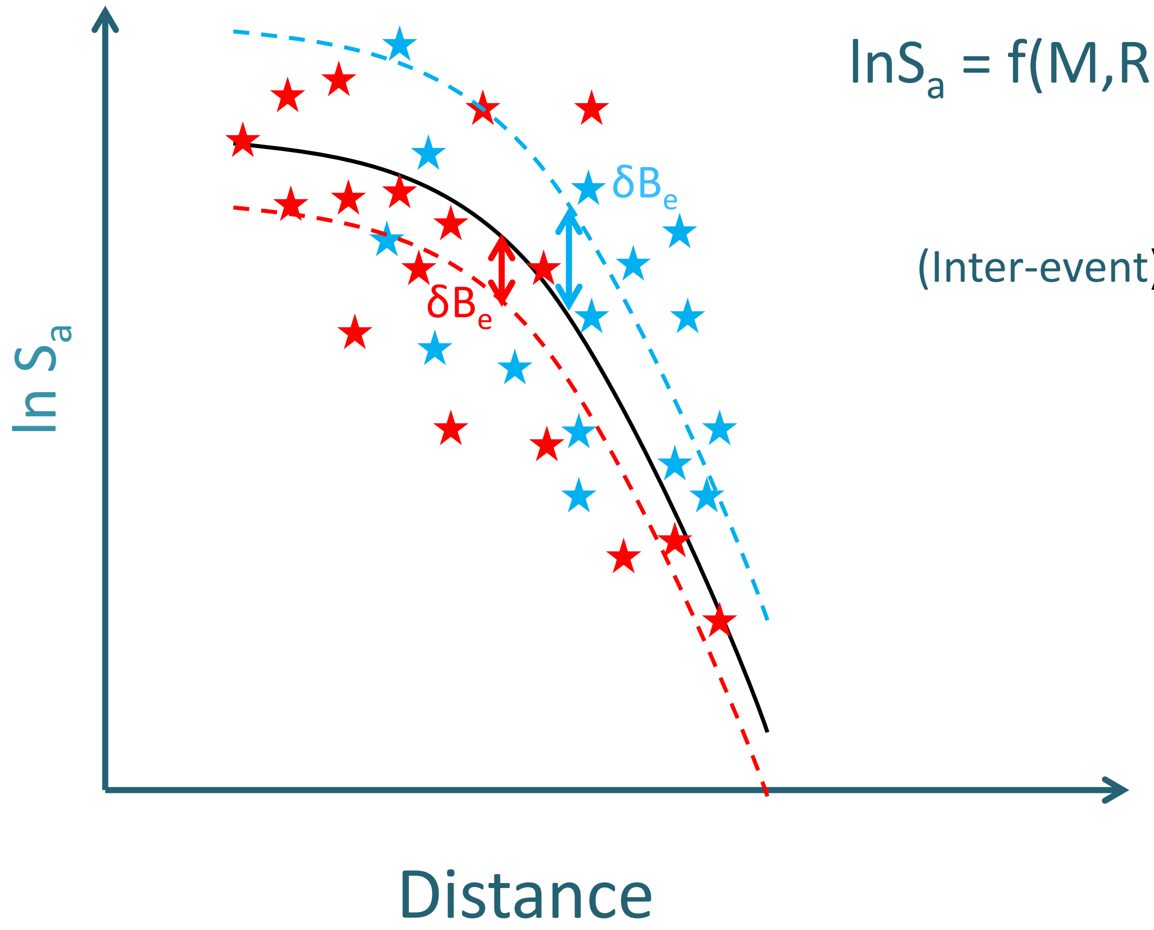

$\ln S_a = f(M,R\ldots) + \Delta$

↓

(Inter-event) $\delta B_e + \delta W_{es}$ (Intra-event)

Residual Partitioning

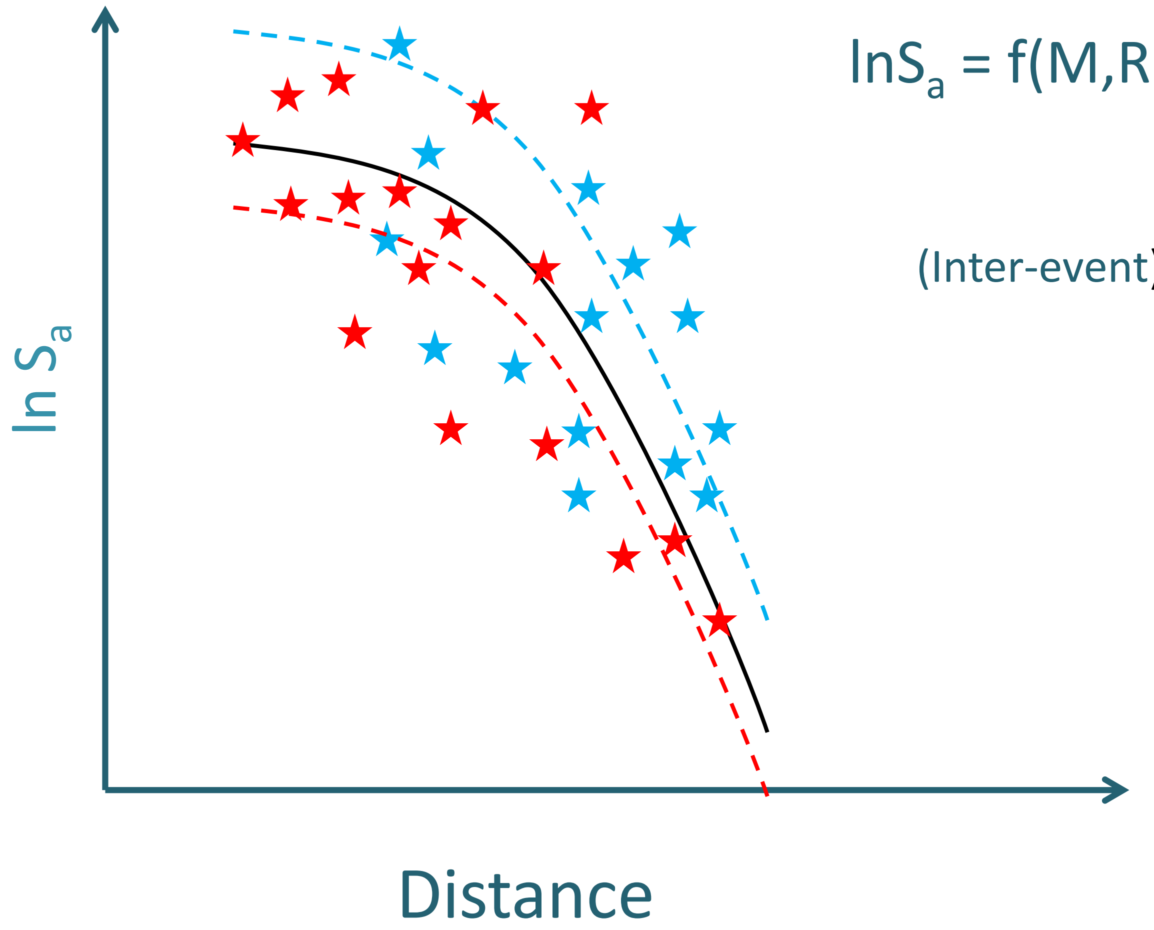

$\ln S_a = f(M,R\ldots) + \Delta$

↓

(Inter-event) $\delta B_e + \delta W_{es}$ (Intra-event)

Residual Partitioning

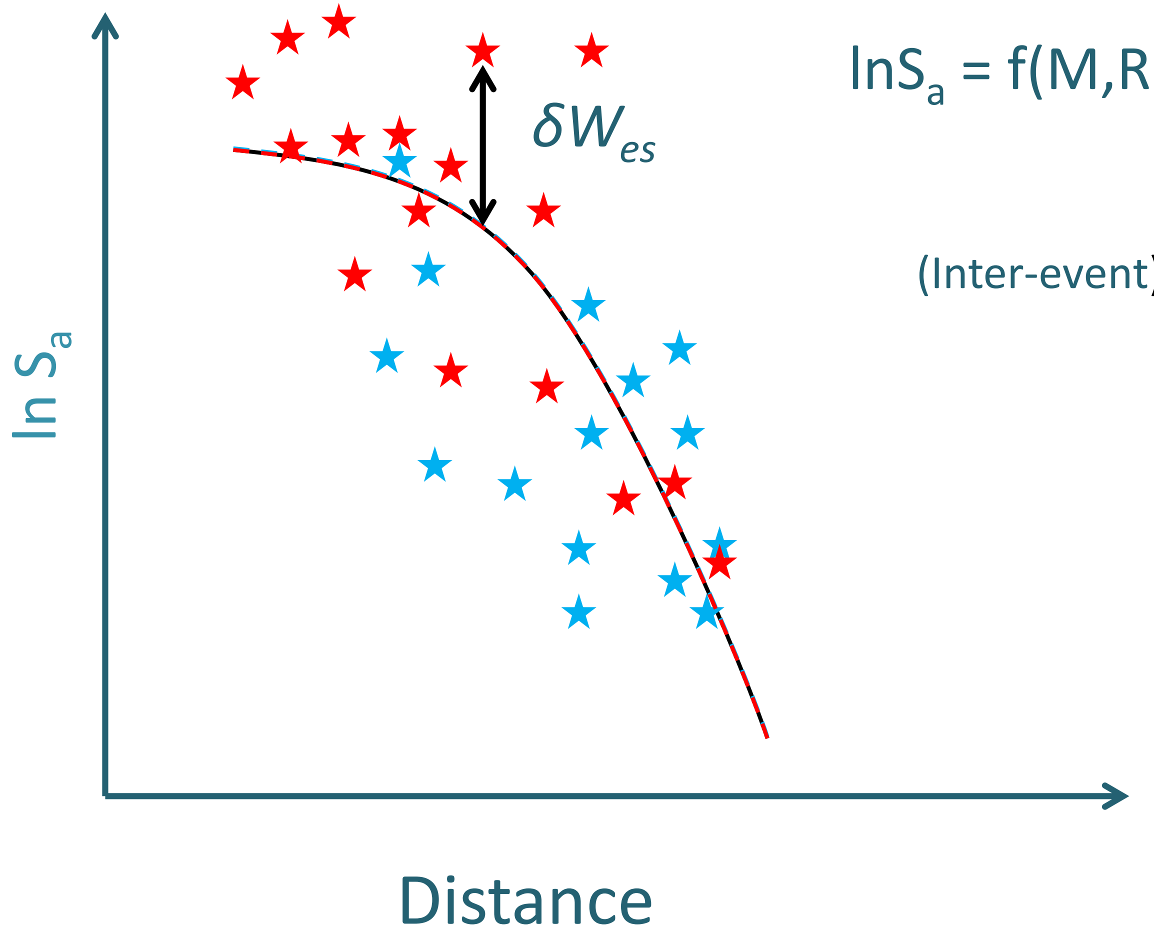

$\ln S_a = f(M,R\ldots) + \Delta$

↓

(Inter-event) $\delta B_e + \delta W_{es}$ (Intra-event)

Residual Partitioning

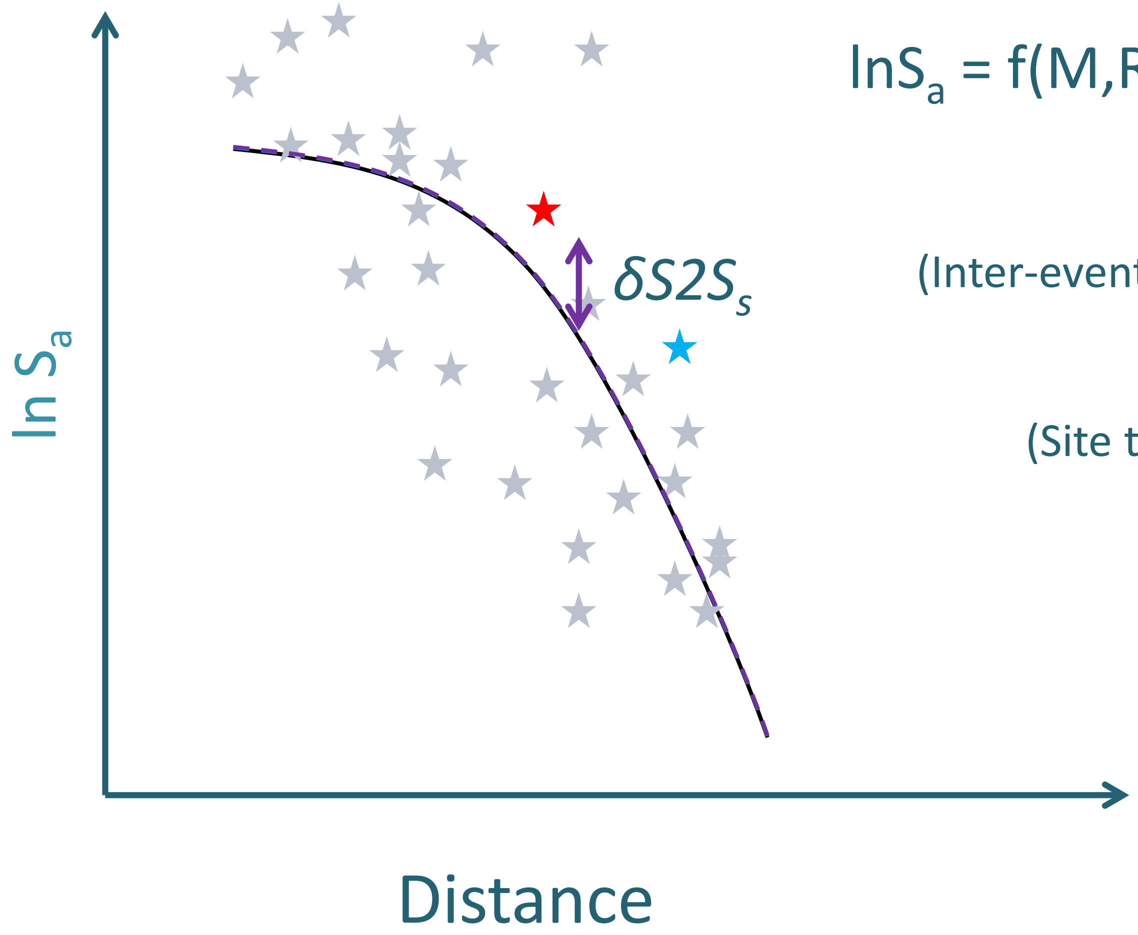

$\ln S_a = f(M,R\ldots) + \Delta$

↓

(Inter-event) $\delta B_e + \delta W_{es}$ (Intra-event)

↓

(Site term) $\delta S2S_s + \delta WS_{es}$

(Site-and-event corrected)

Residual Analysis: Terrain

Relative elevation Smoothed slope Smoothed curvature

Residual Analysis: Terrain

$\delta W_{es} = \delta S2S_s + \delta WS_{es}$

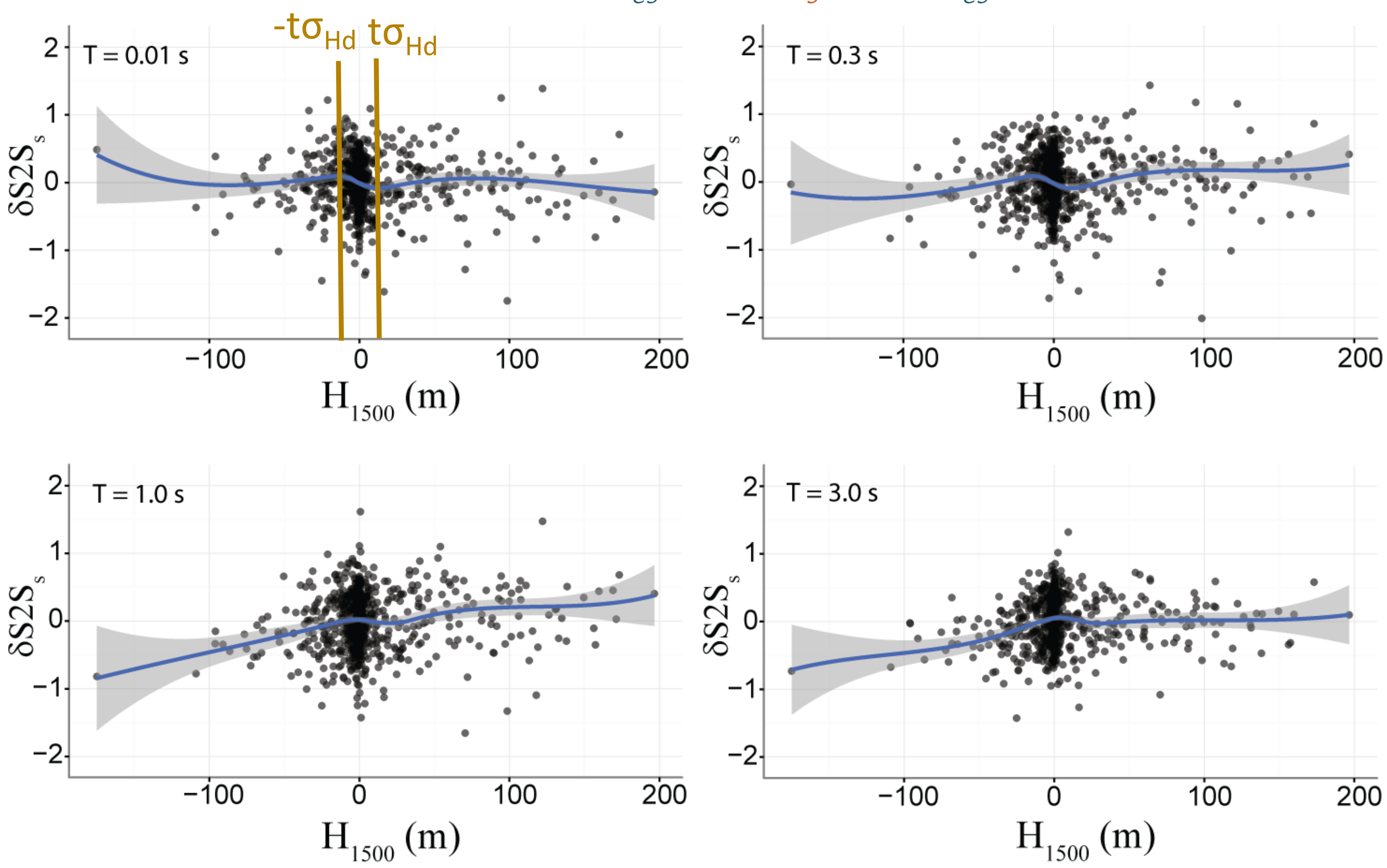

Residual Analysis: Terrain

$\delta W_{es} = \delta S2S_s + \delta WS_{es}$

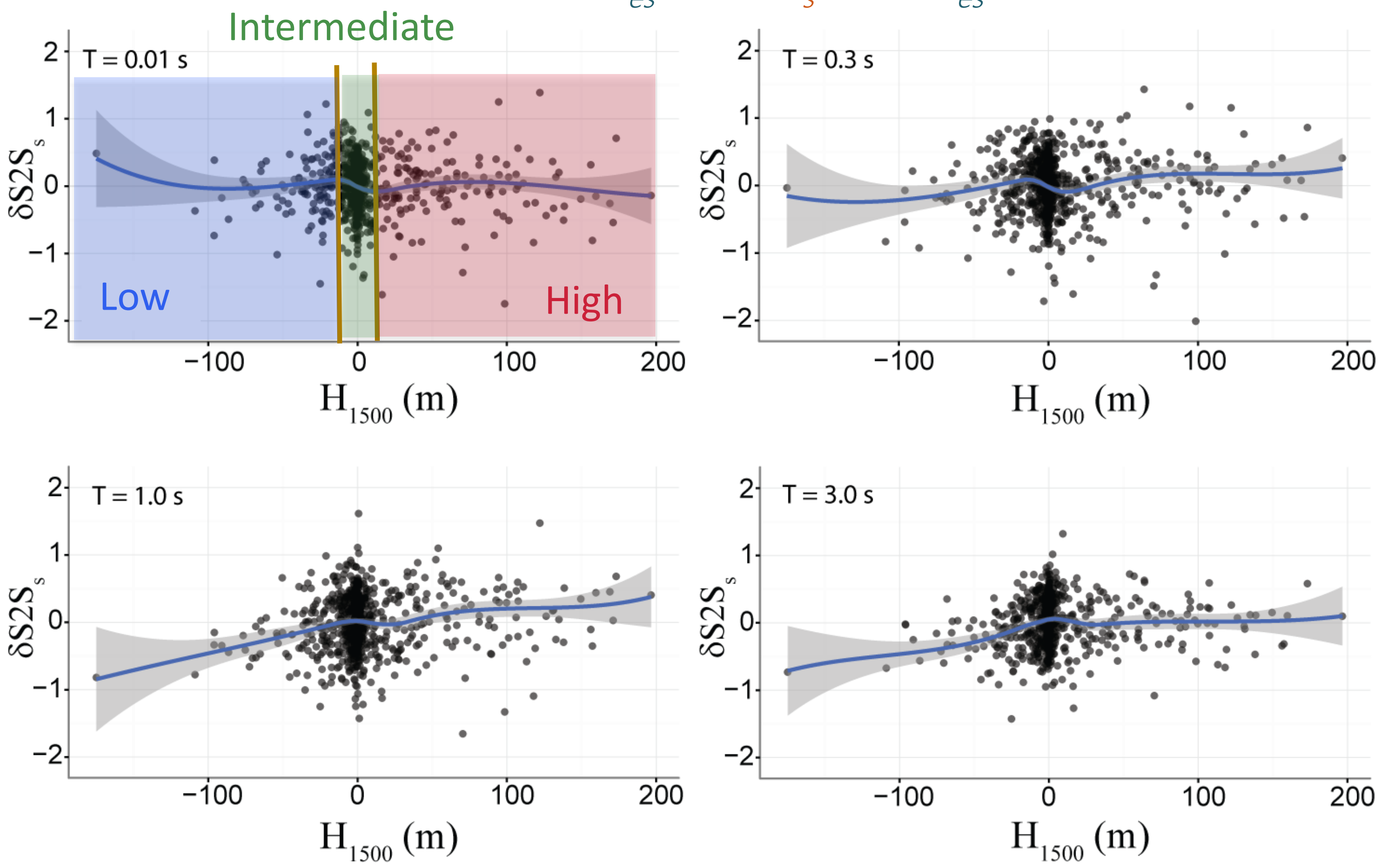

Residual Analysis: Terrain

$$\delta W_{es} = \delta S2S_s + \delta WS_{es}$$

$$\overline{\delta S2S_s} = mean\ (\delta S2S_s)$$

High: $H_d > t\sigma_{Hd}$
Low : $H_d < -t\sigma_{Hd}$

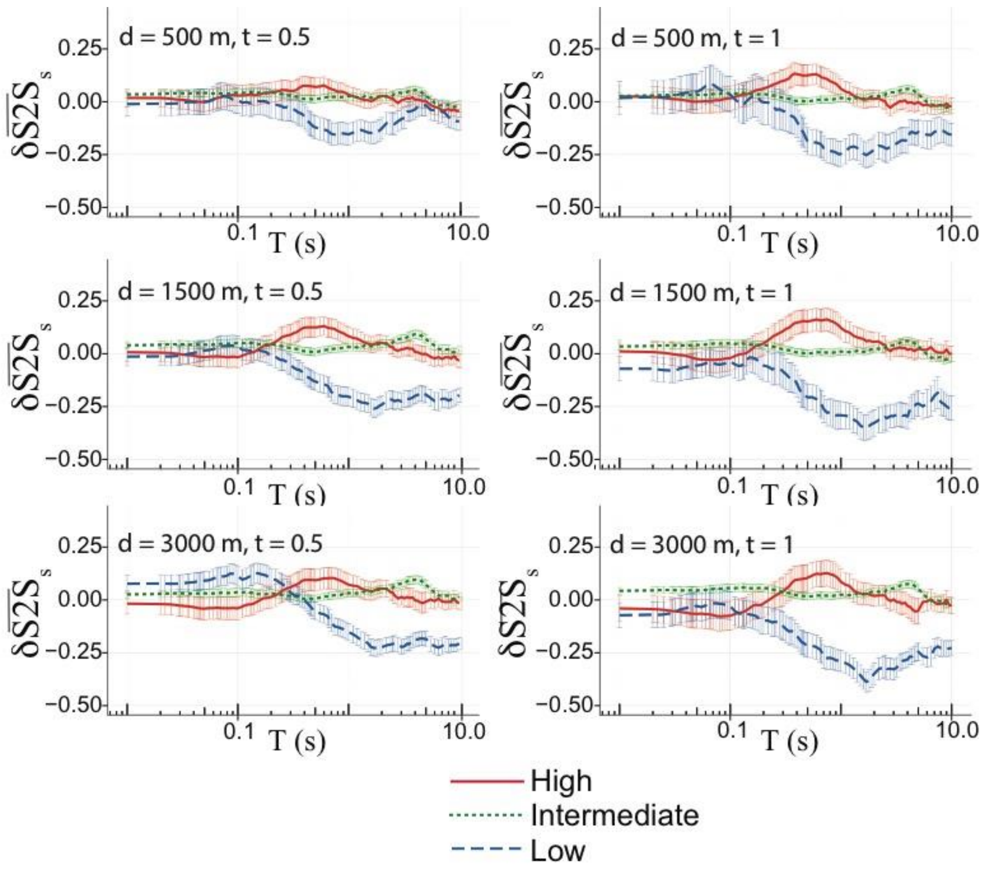

Differences in classes (High, Intermediate, Low) are statistically significant for some period band and some scales

Residual Analysis: Terrain

$\delta W_{es} = \delta S2S_s + \delta WS_{es}$

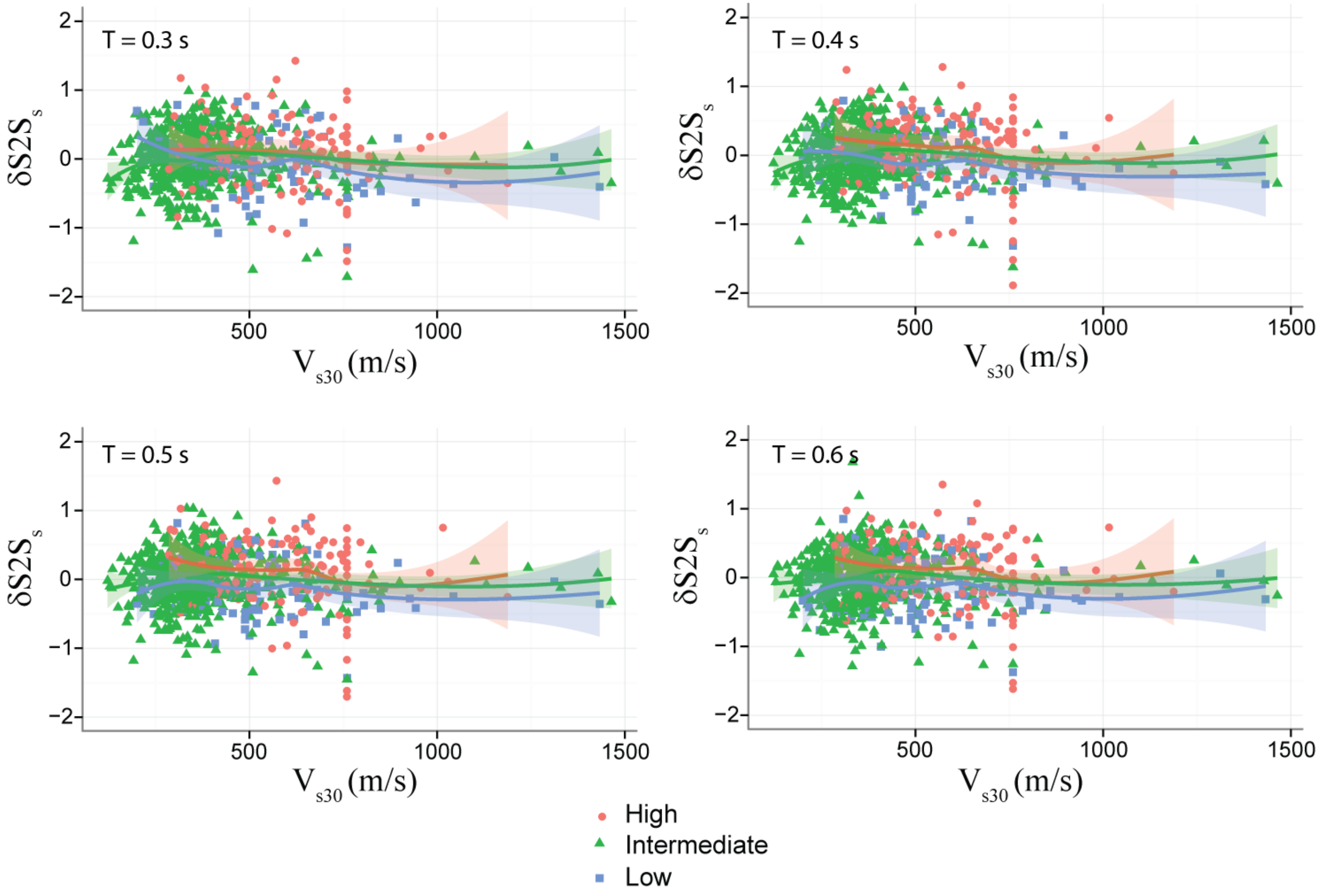

No correlation of different classes with Vs30

Residual Analyses: Terrain

- The optimal smoothing scale is proportional to the oscillator period
  - Except at short periods, where topographic amplification is not seen in the data
- For simplicity – one scale (1500m) selected
  - Captures better the "high" class

Spectral Period (s)	Scale (m)		
	500	1500	3000
0.01	0.0094	-0.0346	-0.0636
0.05	-0.0242	-0.0642	-0.0935
0.1	-0.013	-0.0663	-0.0975
0.15	0.0078	-0.0465	-0.0708
0.2	0.0423	-0.0117	-0.0379
0.25	0.0767	0.0301	0.0016
0.3	0.0976	0.0582	0.0299
0.4	0.1445	0.1088	0.0787
0.5	0.1596	0.1331	0.1077
0.6	0.1627	0.1461	0.1248
0.75	0.1541	0.159	0.1504
1	0.1232	0.134	0.1308
1.5	0.0911	0.1259	0.1396
2	0.0818	0.1156	0.1411
3	0.0514	0.0942	0.1193
4	0.0335	0.0726	0.0911
5	0.0392	0.0691	0.086
7.5	0.0359	0.0842	0.1087
10	0.0779	0.1206	0.1419

Correlation coefficients values between the site residuals and the relative elevation parameters computed at scales of 500 m, 1500 m, and 3000 m

Residual Analysis: Terrain

$$\delta W_{es} = \delta S2S_s + \delta WS_{es}$$

$$\overline{\delta S2S_s} = mean\ (\delta S2S_s)$$

High: $H_d > t\sigma_{Hd}$
Low : $H_d < -t\sigma_{Hd}$

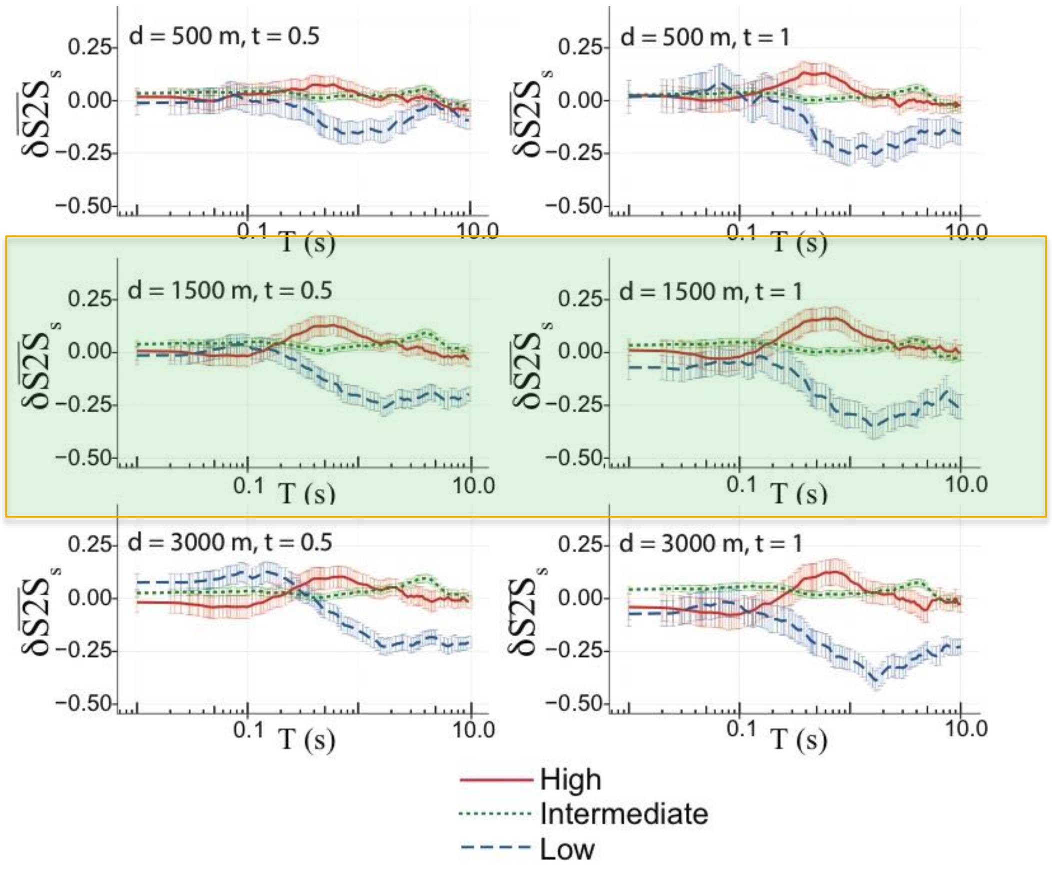

Regression: Terrain

- Fit multi-linear model using linear mixed effects regression:
  - $\delta W_{es} = f_{topo}(H_{1500}) + \delta S2S_s + \delta WS_{es}$

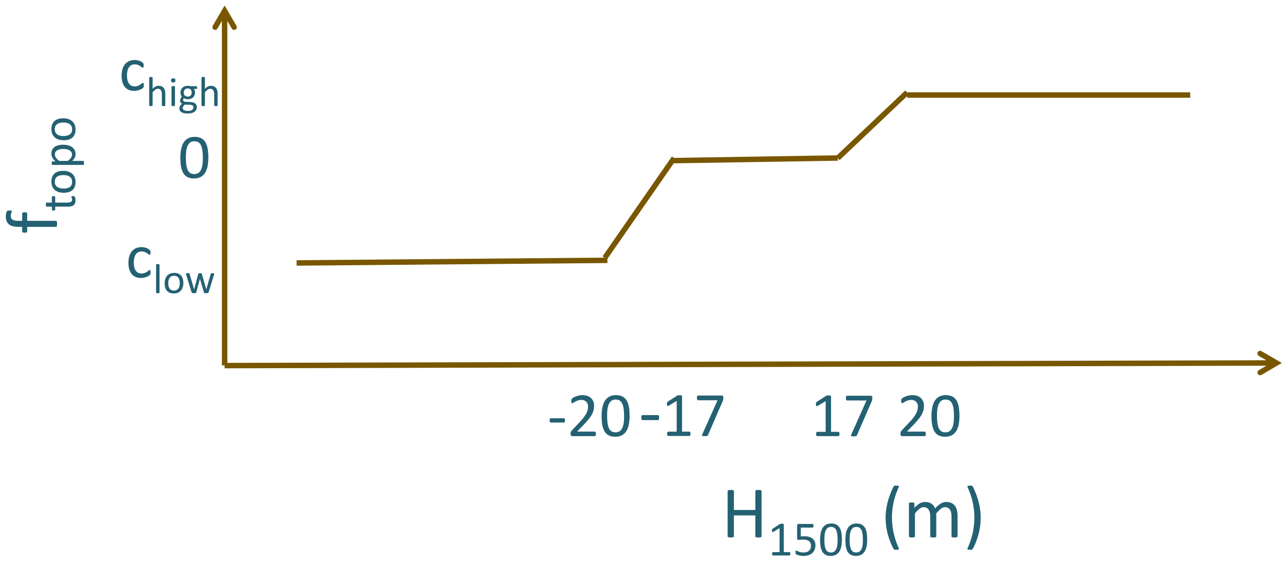

Proposed model: Terrain

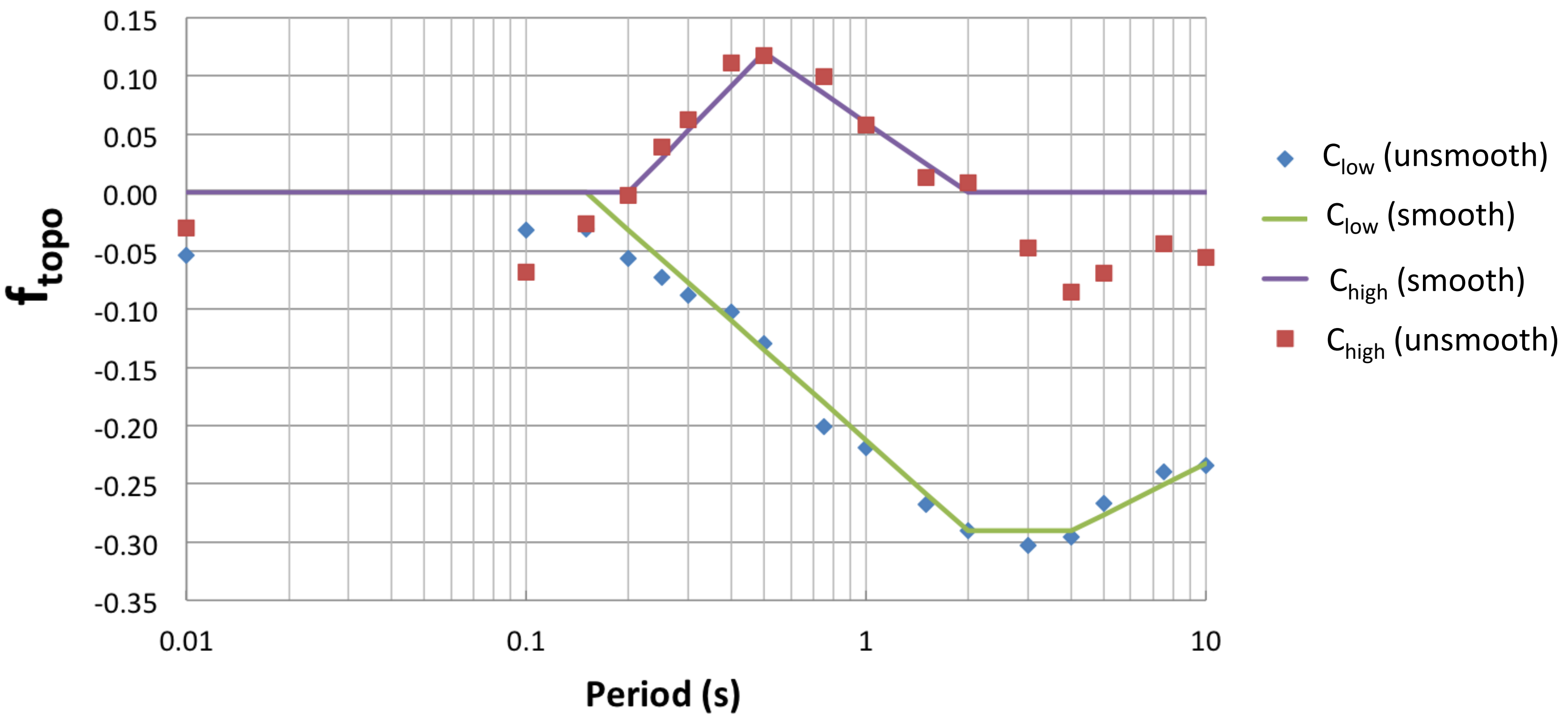

Residuals

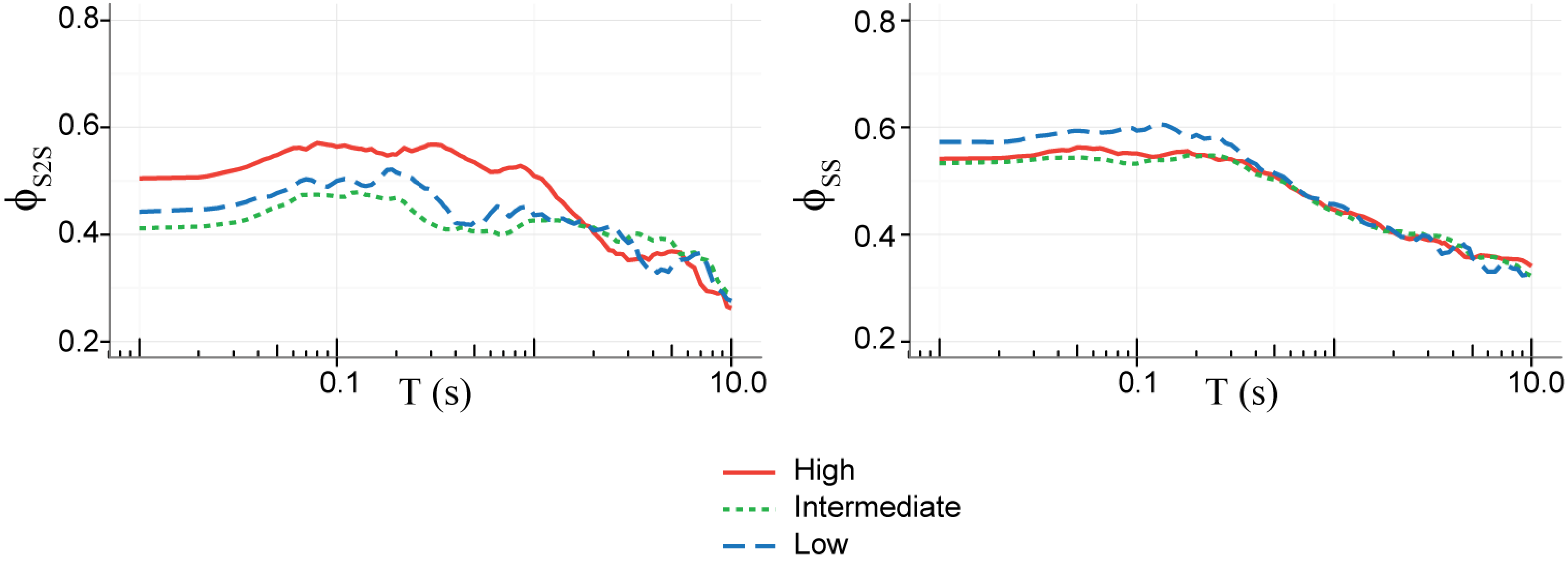

- More site-to-site variability for sites on topography
- Higher single-station standard deviation for sites classified as "low"

Residual Analysis: Terrain

$\delta W_{es} = \delta S2S_s + \delta WS_{es}$

T = 0.5 s

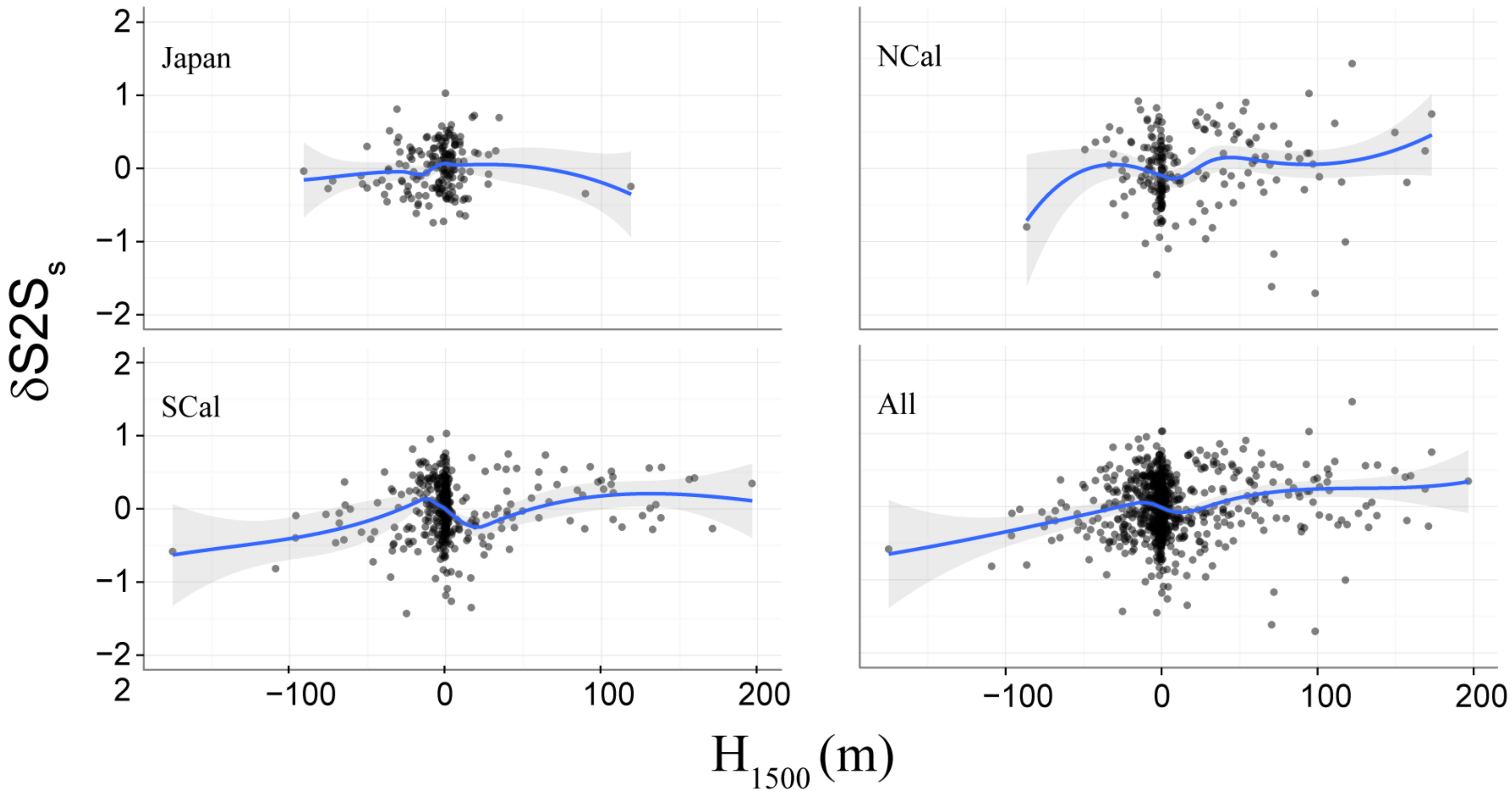

Warning: Does not work equally well in all regions

Residual Analysis: Numerical

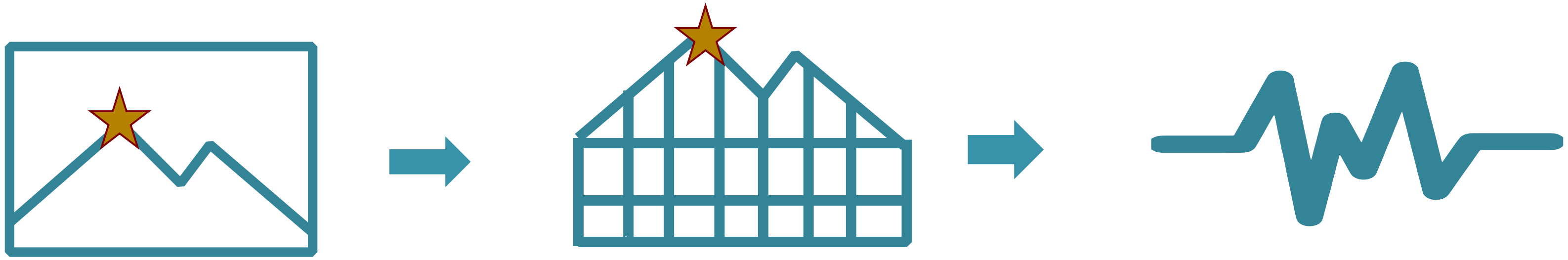

X- sections

FLAC meshes

Output time
histories from
FLAC

Residual Analysis: Numerical

- 2 approaches
  - Constant V_s of 500 m/s
  - $V_s = V_{s30}$
- 3 periods of input harmonic waves
  - T = 0.5 s, 1 s, and 2 s
- 6 orientations : Use natural log of Normalized PGA (lnAmp) to develop family of parameters
  - Maximum, Minimum, Average
  - Parallel
  - Perpendicular

Residual Analysis: Numerical

- Compare predictive power of different lnAmp parameters
  - Fit loess models to the intra-event residuals with respect to all lnAmp parameters
  - Compare R^2 values from different regressions
    - R^2 is coefficient of determination
    - Quantifies goodness of fit of a regression to the data

Residual Analysis: Numerical

Approach 1, constant V_s of 500 m/s

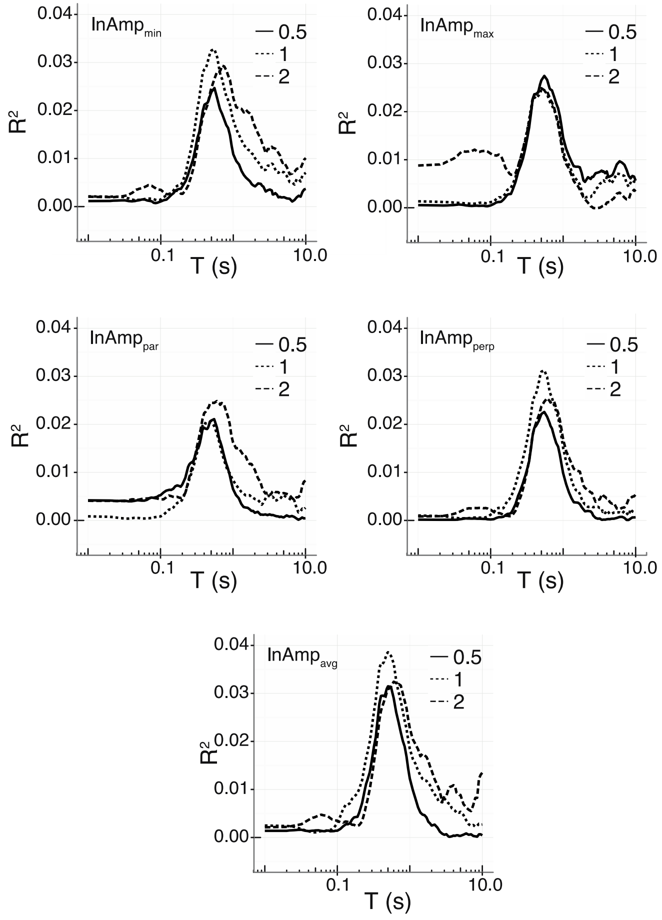

Approach 2, V_s of V_{s30}

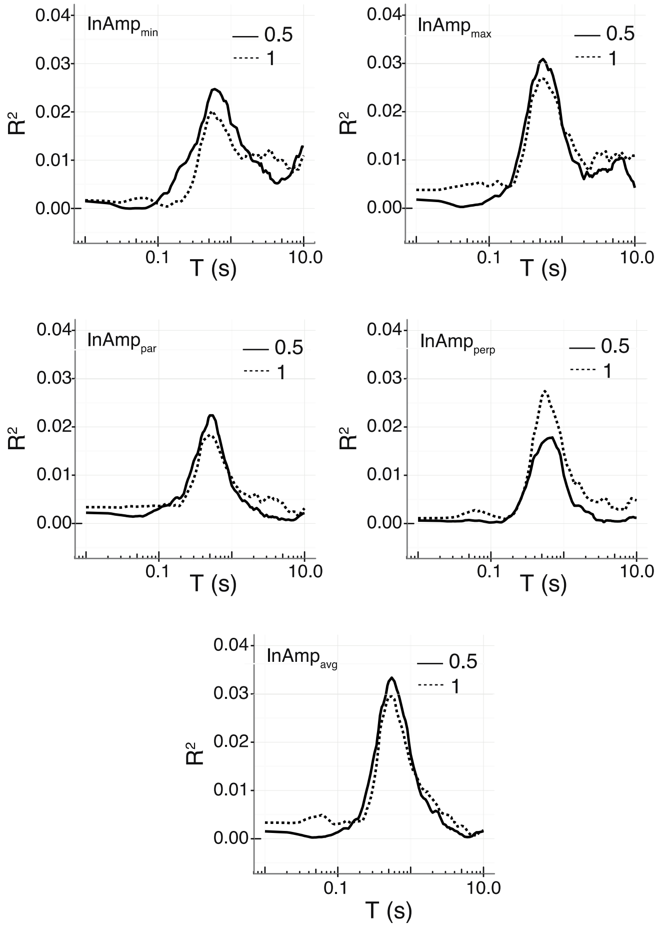

Comparison: Terrain and Numerical Parameters

$\ln Amp_{avg}$ = mean (ln(Normalized PGA) from 6 orientations)

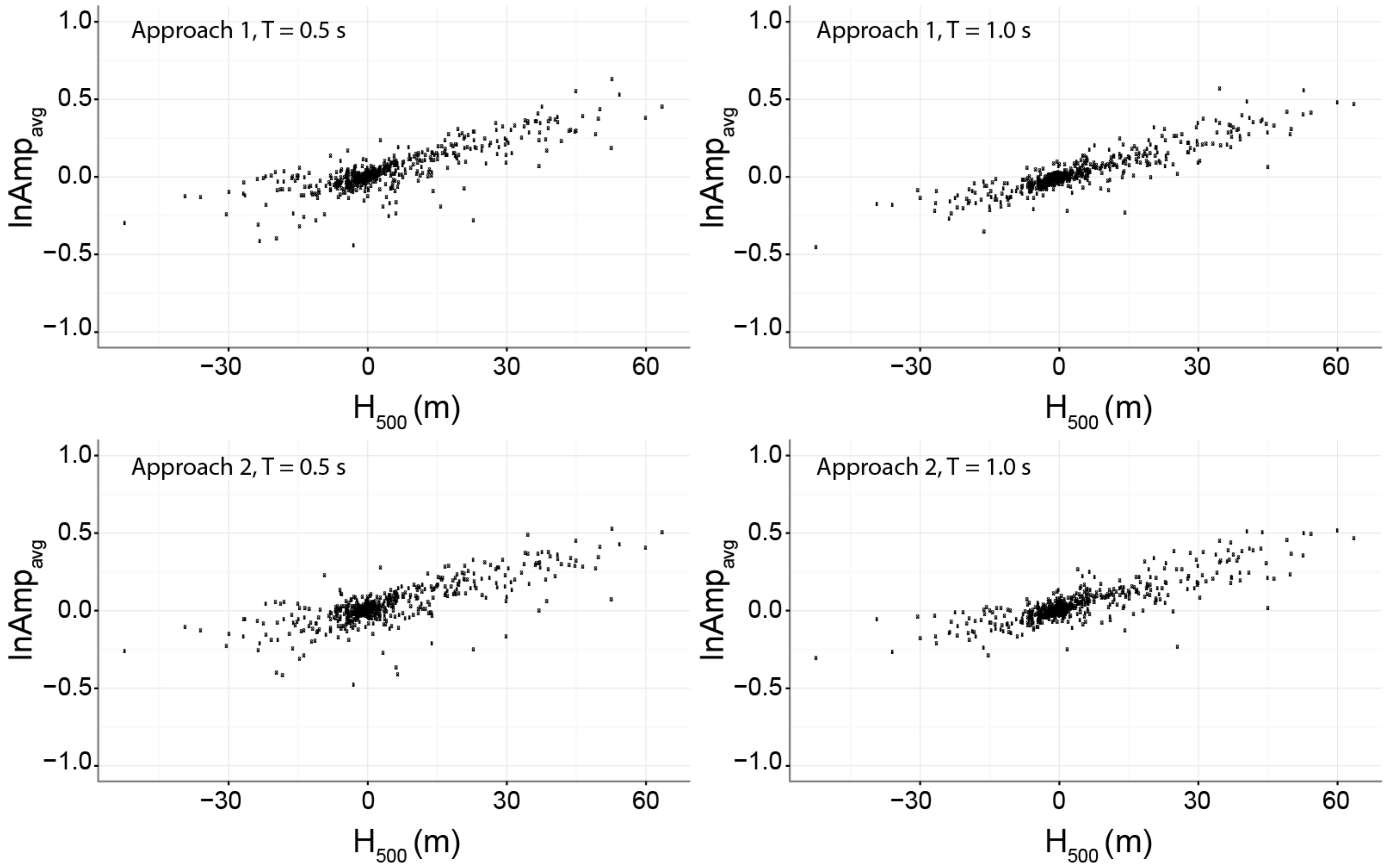

Comparison: Terrain and Numerical Parameters

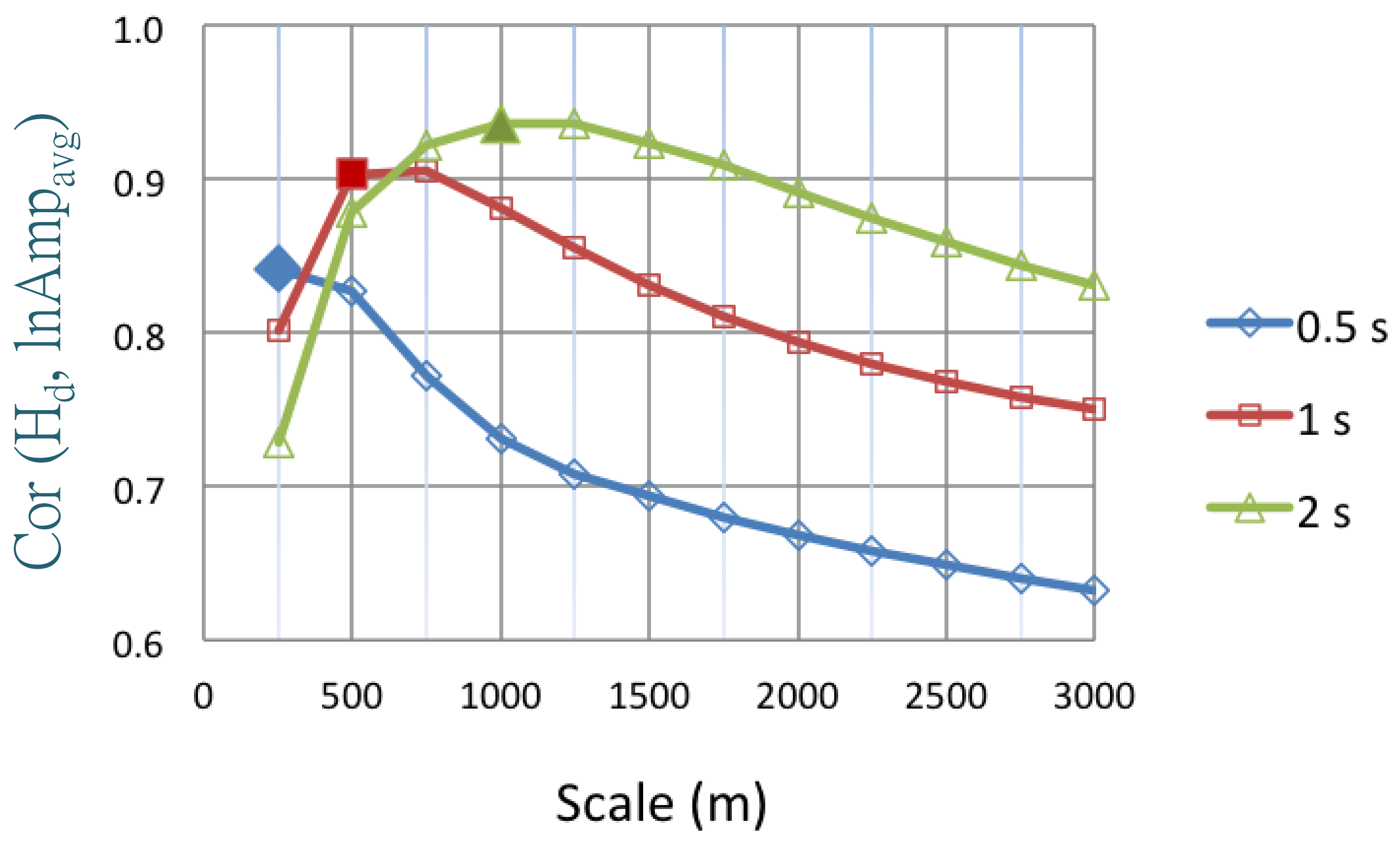

Comparison: Terrain and Numerical Parameters

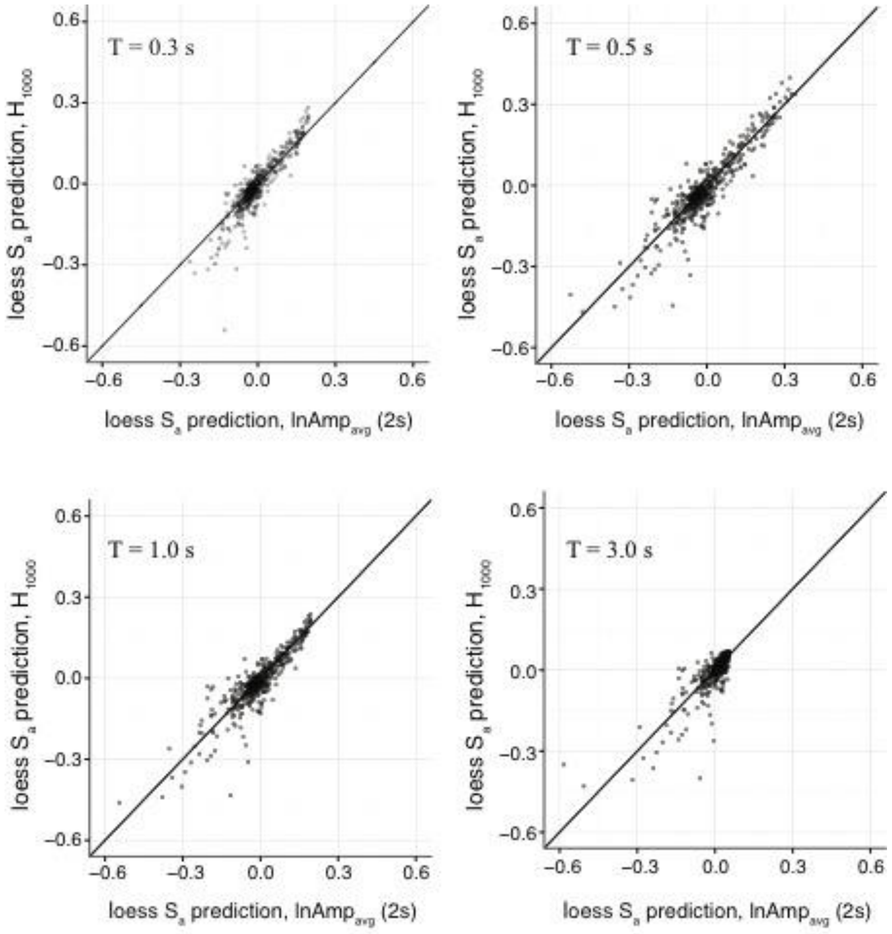

Comparison: Terrain and Numerical Parameters

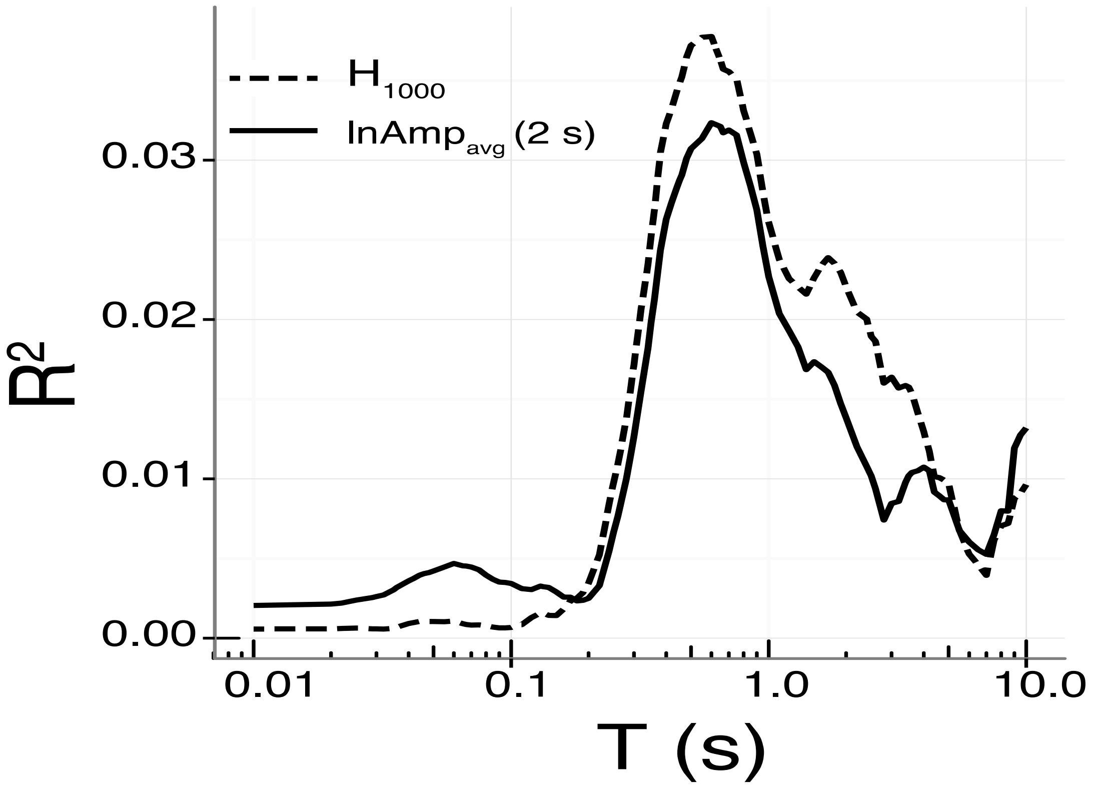

SUMMARY AND CONCLUSIONS

Summary and Conclusions

- Numerical-based parameters perform equally well than geometry-based parameters (e.g., H_d)
  - Shows that H_d captures topographically-related effectds

Summary and Conclusions

- Relative elevation can capture topographic biases in the residuals
  - Amplifications of about 13 % were observed for high sites at T = 0.5 s
  - De-amplification of about 25% for low sites at T = 2 – 4 s
- A parameter based on 2D numerical analyses does equally well, but not better
  - Geometry-based parameter is simpler to compute

Significance of this work

- An empirical model to predict topographic effects
- Significantly reduce prediction biases
- Findings can directly be used by ground motion modelers to improve next generation ground models

Future work

- Study other datasets
- Implement model in GMPE development
- Topographic effects on vertical motion
- Study site terms in Fourier Amplitude-based GMPEs

Publications

- Rai, M., Rodriguez-Marek, A., and Chiou, B.S. (2017). "Empirical terrain-based topographic correction factors for use in ground motion prediction," *Earthquake Spectra* 33(1), 157-177. DOI: 10.1193/071015EQS111M.
- Rai, M., Rodriguez-Marek, A., and Asimaki, D. (2016). "Topographic proxies from 2-D numerical analyses." *Bulletin of Earthquake Engineering* 14, 2959-2975. DOI: 10.1007/s10518-016-9933-4.
- Rai, M., Rodriguez-Marek, A., and Yong, A. (2016). "An empirical model to predict topographic effects in strong ground motion using California small to medium magnitude earthquake database," *Earthquake Spectra*, 32(2), 1033-1054. DOI: http://dx.doi.org/10.1193/113014EQS202M
- Rai, M., Rodriguez-Marek, A., and Yong, A. (2012). "Topographic effects in strong ground motion." 15 World Conference on Earthquake Engineering, Lisbon, September 2012.
- Rai, M., and Rodriguez-Marek, A. (2014). Parameterization of topography for ground motion prediction equations," Proceedings of the SMIP14 Seminar on Utilization of Strong Motion Data, Berkeley, CA, October 9.

Acknowledgements

- Dr. Manisha Rai
- Co-authors
  - Brian Chiou, Alan Yong, Domniki Assimaki
- CSMIP and NSF
- NSF Topo team:
  - Pis: D. Asimaki, B. Cox, J. Wartman, M. Pando
  - Ph.D. Students: Jake Dafni, Jeokho Seong, Clinton Wood, Manisha Rai

THANKS